

Experimental results on TMDs

H. Avakian¹, A. Bressan², and M. Contalbrigo^a

¹ Jefferson Lab

² University of Trieste and INFN

³ University of Ferrara and INFN

Received: date / Revised version: date

Abstract. QCD factorisation for semi-inclusive deep inelastic scattering at low transverse momentum in the current-fragmentation region has been established recently, providing a rigorous basis to study the Transverse Momentum Dependent distribution and fragmentation functions (TMDs) of partons from Semi-Inclusive DIS data using different spin-dependent and spin-independent observables. The main focus of the experiments were the measurements of various single- and double-spin asymmetries in hadron electro-production ($ep^\uparrow \rightarrow ehX$) with unpolarised, longitudinally and transversely polarised targets. The joint use of a longitudinally polarised beam and longitudinally and transversely polarised targets allowed to measure double-spin asymmetries (DSA) related to leading-twist distribution functions describing the transverse momentum distribution of longitudinally and transversely polarised quarks in a longitudinally and transversely polarised nucleons (*helicity and worm-gear TMDs*). The single-spin asymmetries (SSA) measured with transversely polarised targets, provided access to a specific leading-twist parton distribution functions: the transversity, the Sivers function and the so-called “pretzelosity” function. In this review we present the current status and some future measurements of TMDs worldwide.

PACS. 13.60.-r Photon and charged-lepton interactions with hadrons – 13.60.Le Meson production

1 Introduction

Since decades, few questions have challenged the interpretation of hadron structure and phenomena in Hadronic Physics in terms of perturbative Quantum Chromodynamics (QCD). Among the most compelling, there are the spin budget of the nucleon (hadrons), where there are missing contributions not quantified yet, and the surprising single-spin asymmetries in hadron reactions, which do not vanish as expected with increasing energy. The questions above relate to one of the fundamental degree of freedom of the elementary particles, the spin, and its correlation with the motion (i.e. transverse momentum) of the partons.

As part of the most general mechanism of confinement, these correlations might manifest also in unpolarised reactions where particle polarisation is not directly observed or controlled. Relevant examples are the azimuthal asymmetries of hadrons produced in opposite hemispheres at the e^+e^- colliders [1] or responsible of the Lam-Tung relation violation in Drell-Yan production [2]. Such correlations might influence the low transverse momentum distribution of topical particles, i.e. (vector) bosons, pro-

duced at hadronic colliders, and has to be taken into account for precision measurements.

Most of our present understanding of the internal structure of nucleons derives from inclusive deep inelastic scattering (DIS) experiments performed over the past four decades in different kinematic regimes at fixed-target experiments and collider machines. Based on the large amount of precise data provided by these experiments we have reached a good knowledge of the parton longitudinal-momentum and longitudinal-spin distributions of quarks in the nucleon. Such investigation is based on the so-called collinear factorization of the cross-section into non-perturbative parton distribution functions (PDFs) and fragmentation functions (FFs), a mono-dimensional approach where the given longitudinal direction is the one of the hard probe (the exchanged virtual boson).

In the recent years, new Transverse Momentum Dependent (TMD) parton distributions and fragmentation functions, in this work abbreviate as TMDs for simplicity, have been introduced to describe the rich complexity of the hadron structure, taking into account the parton transverse degrees of freedom and moving toward the achievement of a 3D comprehension of the parton dynamics. At the same time new channels of investigation have been gaining importance as the study of semi-inclusive deep-inelastic-scattering (SIDIS) reactions where the hadron

Send offprint requests to:

^a Present address: Insert the address here if needed

produced by the struck quark is observed in conjunction with the scattered lepton probe. Such measurements have become possible by the parallel evolution of the experimental apparatuses.

It is being realized that in DIS reactions, single and dihadron semi-inclusive and hard exclusive production, both in current and target fragmentation regions, provide a variety of spin and azimuthal angle dependent observables sensitive to the dynamics of quark-gluon interactions. Studies of the parton distribution functions which encode transverse momentum (TMDs) or transverse position (GPDs) [3] information is gathering increasing interest, are currently driving the upgrades of several existing facilities (Jefferson Lab, COMPASS and RHIC), and having an important role in the design and construction of new facilities worldwide (EIC, FAIR, NICA and JPARC).

The main objectives of ongoing and future studies of TMDs is the understanding of the internal structure of the nucleon and nucleus and hadron formation in terms of quarks and gluons, the fundamental degrees of freedom of QCD. At the price of an unprecedented complexity, the novel paradigm of hadron structure TMD investigation may eventually shed new light on the phenomena of quark confinement as it connects, i.e., with colour-glass condensate and quark propagation in cold nuclear matter, see Section 3.1.

This work presents a selection of available observations and upcoming measurements planned in SIDIS experiments to address the mysteries of the hadron structure from a modern point of view.

2 Transverse Momentum Parton Distributions and Fragmentation Functions

The quark-gluon dynamics can be described by a set of non-perturbative functions describing all possible spin-spin and spin-orbit correlations. In an operator product expansion (OPE) of the scattering amplitude, the twist is used to classify the operators and isolate the leading contributions, at twist-2, from the subleading higher-twist contributions, power suppressed as $Q^{2-\text{twist}}$. The eight leading-twist transverse momentum dependent parton distribution functions (TMD-PDFs) are listed in Table 1, for different combinations of nucleon and quark spin orientations. The TMD-PDFs carry information not only on the longitudinal but also on the transverse momentum of partons, providing rich and direct information on the orbital motion of quarks [4–14] (see Table 1). They are all independent functions although possible relationships can be found depending on model-dependent assumptions.

The diagonal elements are the momentum distribution $f_1(x, k_\perp)$, the helicity distribution $g_1(x, k_\perp)$, and the presently poorly known transversity distribution $h_1(x, k_\perp)$. Here x denotes the longitudinal momentum fraction carried by the partons and the scale dependence on Q^2 (the negative squared four-momentum of the exchanged virtual boson) has been neglected for simplicity. These functions do not vanish when integrated in the transverse quark momentum k_\perp and can thus be studied in the collinear limit,

Table 1. Leading-twist transverse momentum-dependent distribution functions. The symbols U , L , and T stand for transitions of unpolarised, longitudinally polarised, and transversely polarised nucleons N (rows) to corresponding quarks q (columns).

N/q	U	L	T
U	f_1		h_1^\perp
L		g_1	h_{1L}^\perp
T	f_{1T}^\perp	g_{1T}^\perp	h_1 h_{1T}^\perp

as was widely done in the past for the momentum and helicity distribution.

The TMD distributions for transversely polarised quarks arise from interference between amplitudes with left- and right-handed polarisation states, and only exist because of chiral symmetry breaking in the nucleon wave function in QCD. Their study therefore provides a new avenue for probing the chiral nature of the partonic structure of hadrons. For example, the transversity distribution reflects the quark transverse polarisation in a transversely polarised nucleon and is related to the tensor charge of the nucleon [15, 16]. Although fundamental for the nucleon description, transversity has long remained unmeasured due to its chirally-odd nature, which prevents its measurement in inclusive DIS: the transversity distribution can only be measured in conjunction with another chiral-odd object. One possibility is represented by SIDIS reactions, where at least one final state hadron is detected in coincidence with the scattered lepton, thus conjugating parton distribution with fragmentation functions.

Off-diagonal elements are genuine transverse momentum dependent functions which vanish after k_\perp integration. They require non-zero orbital angular momentum as they are related to the wave function overlap of nucleon Fock states with different angular momentum. The chiral-even distributions $f_{1T}^\perp(x, k_\perp)$ and $g_{1T}^\perp(x, k_\perp)$ are the imaginary parts and the chiral-odd $h_1^\perp(x, k_\perp)$ and $h_{1L}^\perp(x, k_\perp)$ are the real parts of the interference terms between S and P wave components. The chiral-odd $h_{1T}^\perp(x, k_\perp)$ function is sensitive to the D -wave component.

Among the most intriguing parton functions, the TMD $f_{1T}^\perp(x, k_\perp)$ and $h_1^\perp(x, k_\perp)$ parton distributions are known as the Sivers [5] and Boer-Mulders [8] functions. As a consequence of a non-trivial gauge link required for their gauge-invariant definition, they are naively T -odd (do not violate T -invariance due to the interaction phase) and exhibit a peculiar process dependence: a sign change is expected moving from SIDIS to Drell-Yan processes, whose verification is one of the most urgent goals of the present experimental activity. The Sivers and Boer-Mulders functions describe unpolarised quarks in the transversely polarised nucleon and transversely polarised quarks in the unpolarised nucleon, respectively. The most simple mechanism that can lead to a Boer-Mulders (Sivers) function is a correlation between the spin of the quarks (nucleon) and the quark orbital angular momentum. In combination

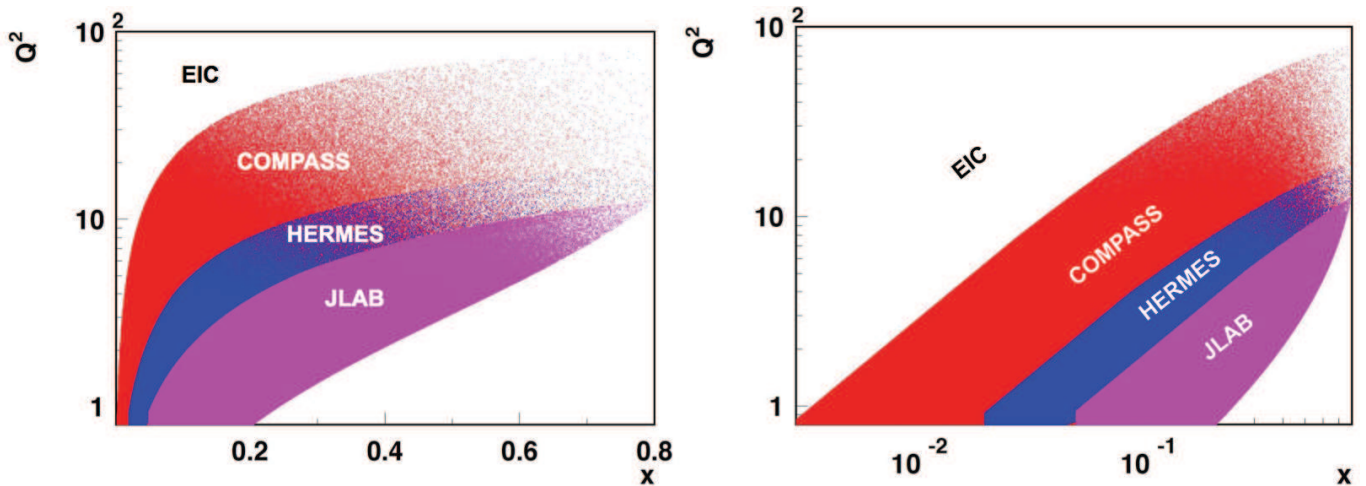


Fig. 1. Kinematic coverage of COMPASS (160 GeV muon beam), HERMES (27 GeV electron beam) and JLab (11 GeV electron beam) showing the complementariness among the experiments. Left and right plots show the detailed coverage in linear-log and log-log scales.

with a final state interaction that is on average attractive, such correlations manifest as azimuthal asymmetries of the produced hadron distribution.

An analogous of Table 1 exists for the fragmentation functions. As the polarisation in the final state is not accounted for in this work, only two transverse momentum dependent fragmentation functions (TMD-FFs) are considered in the following: the unpolarised $D_1(z, p_\perp)$ and the Collins $H_1^\perp(z, p_\perp)$ fragmentation function, where z is the energy fraction carried by the final state hadron and p_\perp is the transverse momentum acquired by the observed hadron with respect to the fragmenting quark. The Collins function acts as a polarimeter being sensitive to the correlation between the transverse momentum gained during fragmentation and the transverse polarisation of the fragmenting quark [17] and allows to access the chirally-odd distribution functions. The measurements indicate a peculiar behaviour of the Collins function, with similar magnitude but opposite sign for favoured (the fragmenting quark is a valence quark of the produced hadron) and unfavoured fragmentation.

TMDs can be accessed in SIDIS through measurements of specific azimuthal angle dependencies of the cross-section. Observables sensitive to those TMDs were under intensive experimental studies at different Laboratories worldwide. Measurements using electro-production of hadrons and focused on TMD studies have been performed by HERMES at HERA, COMPASS at CERN and halls A,B and C at JLab. After the first exploratory phase holding for about a decade, it is now the time of transition to a new precision phase for the exploration of the nucleon 3D structure. In particular, precision measurements of spin and azimuthal asymmetries in pion and kaon SIDIS production off unpolarised, longitudinally polarised and transversely polarised p , d and ^3He targets would allow to extract the spin and flavour dependences of transverse momentum distributions of quarks. The TMDs non-trivial universality properties would be proven by comparing SIDIS re-

sults, i.e. on Sivers function, with measurements in Drell-Yan experiments at COMPASS and W -boson production at RHIC. Combination of measurements in the extended range of momentum transfer Q^2 , covered by the existing and upcoming facilities, would allow studies of Q^2 -dependences of TMDs, for example for the Sivers function, predicted to have very non-trivial evolution properties [18, 19], and the disentanglement of the possible sub-leading contributions. The overlap of kinematical coverages of COMPASS, HERMES and JLab (see Fig. 1) would allow studies of Q^2 -dependence in the range of Bjorken $x \sim 0.1 - 0.2$, where the effects related to orbital motion of quarks are expected to be significant. The coverage in x and Q^2 would be ultimately extended with the realization of an Electron-Ion Collider (EIC), a facility among the recommendations of the US Nuclear Science Advisory Committee 2015 Long Range Plan.

3 Measuring spin-azimuthal asymmetries in SIDIS

In the one-photon exchange approximation valid at the fixed-target experiments, the SIDIS cross section can be decomposed in terms of Structure Functions [11, 20], each related to a specific azimuthal modulation:

where λ_e refers to the helicity of the electron beam, S_L and S_T to the longitudinal and transverse polarisation of the target nucleons (with respect to the direction of the virtual photon), and ϵ to the ratio of the longitudinal and transverse photon fluxes, which is determined by the kinematics of the lepton. Here, $q = \ell - \ell'$ is the four-momentum of the virtual photon, $Q^2 = -q^2$, $x = Q^2/2(P \cdot q)$, $y = (P \cdot q)/(P \cdot \ell)$, ϕ_S is the azimuthal angle of the transverse spin in the scattering plane, and P is the initial nucleon momentum. The azimuthal angle ϕ is defined as the angle

$$\begin{aligned}
\sigma(\phi, \phi_S) \equiv & \frac{d^6\sigma}{dx dy dz d\phi d\phi_S dP_{hT}^2} = \frac{\alpha^2}{xyQ^2} \frac{y^2}{2(1-\epsilon)} \left(1 + \frac{\gamma^2}{2x}\right) \\
& \left\{ F_{UU,T} + \epsilon F_{UU,L} + \sqrt{2\epsilon(1+\epsilon)} \cos\phi F_{UU}^{\cos\phi} + \epsilon \cos(2\phi) F_{UU}^{\cos(2\phi)} + \lambda_e \left[\sqrt{2\epsilon(1-\epsilon)} \sin\phi F_{LU}^{\sin\phi} \right] + \right. \\
& + S_L \left[\sqrt{2\epsilon(1+\epsilon)} \sin\phi F_{UL}^{\sin\phi} + \epsilon \sin(2\phi) F_{UL}^{\sin(2\phi)} \right] + S_L \lambda_e \left[\sqrt{1-\epsilon^2} F_{LL} + \sqrt{2\epsilon(1-\epsilon)} \cos\phi F_{LL}^{\cos\phi} \right] \\
& + |S_T| \left[\sin(\phi - \phi_S) \left(F_{UT,T}^{\sin(\phi-\phi_S)} + \epsilon F_{UT,L}^{\sin(\phi-\phi_S)} \right) + \epsilon \sin(\phi + \phi_S) F_{UT}^{\sin(\phi+\phi_S)} + \epsilon \sin(3\phi - \phi_S) F_{UT}^{\sin(3\phi-\phi_S)} \right. \\
& \left. + \sqrt{2\epsilon(1+\epsilon)} \sin\phi_S F_{UT}^{\sin\phi_S} + \sqrt{2\epsilon(1+\epsilon)} \sin(2\phi - \phi_S) F_{UT}^{\sin(2\phi-\phi_S)} \right] \\
& \left. + |S_T| \lambda_e \left[\sqrt{1-\epsilon^2} \cos(\phi - \phi_S) F_{LT}^{\cos(\phi-\phi_S)} + \sqrt{2\epsilon(1-\epsilon)} \cos\phi_S F_{LT}^{\cos\phi_S} + \sqrt{2\epsilon(1-\epsilon)} \cos(2\phi - \phi_S) F_{LT}^{\cos(2\phi-\phi_S)} \right] \right\}, (1)
\end{aligned}$$

between the scattering plane, formed by the initial and final momenta of the electron, and the production plane, formed by the transverse momentum P_{hT} of the observed hadron and the virtual photon (Fig. 2). The azimuthal angle ϕ_S is defined as the angle between the scattering plane and the target spin component transverse to the virtual photon.

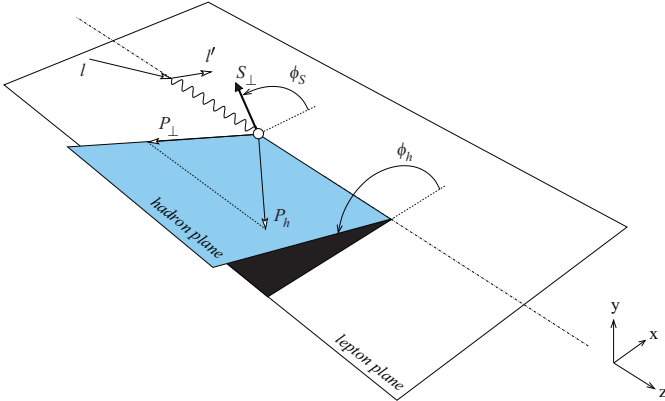


Fig. 2. The SIDIS kinematics.

The subscripts in the structure functions $F_{UT,UL,LT}$, specify the beam (first index) and target (second index) polarisation (U, L, T for unpolarised, longitudinally and transversely polarised targets, and U, L for unpolarised and longitudinally polarised beam). When present, the third index refers to the virtual photon polarisation.

In the regime where the transverse momenta (set by the confinement scale) are small with respect the hard scale Q , the structure functions can be factorised into TMD parton distribution and fragmentation functions, and soft and hard parts [20,21]. At leading-twist (not suppressed by powers of the hard scale Q) there are eight contributions related to the parton distributions in Table 1. They all can be independently measured in SIDIS with different combinations of polarisation states of the incom-

ing lepton and the target nucleon thanks to their specific azimuthal dependencies.

For example with an unpolarised beam and a transversely polarised target one can get access to the structure function $F_{UT}^{\sin(\phi+\phi_S)}(x, z, P_{hT}, Q^2)$. The latter can be written as a convolution of $h_1(x, k_\perp, Q^2)$ and $H_1^\perp(z, p_\perp, Q^2)$, integrated over the transverse momentum of the initial, k_\perp , and fragmenting p_\perp partons:

$$F_{UT}^{\sin(\phi+\phi_S)}(x, y, P_{hT}) = C \left[w(\mathbf{p}_\perp, \mathbf{k}_\perp) h_1^\perp(x, k_\perp) H_1^\perp(z, p_\perp) \right] \quad (2)$$

where the scale dependence has been dropped for simplicity. The convolution integral

$$C[w h_1^\perp H_1^\perp] = x \sum_q e_q^2 \int \delta^2(\mathbf{p}_\perp - z \mathbf{k}_\perp - \mathbf{P}_{hT}) w(\mathbf{p}_\perp, \mathbf{k}_\perp) h_1^{\perp,q}(x, k_\perp) H_1^{\perp,q}(z, p_\perp) d\mathbf{p}_\perp^2 d\mathbf{k}_\perp^2 \quad (3)$$

embeds a summation over quarks and antiquarks, a kinematic prefactor $w(\mathbf{p}_\perp, \mathbf{k}_\perp)$ specific for each structure function (in this case $w(\mathbf{p}_\perp, \mathbf{k}_\perp) = -(\hat{\mathbf{h}} \cdot \mathbf{k}_T)/M_h$ with $\hat{\mathbf{h}} = \mathbf{P}_{hT}/|\mathbf{P}_{hT}|$ the unit vector along the transverse momentum and M_h the mass of the observed hadron), and a delta function imposing momentum conservation $\mathbf{P}_{hT} = z \mathbf{k}_\perp + \mathbf{p}_\perp$ (valid up to order k_\perp/Q).

The Fourier decomposition of the SIDIS cross section and the convolution integrals over the transverse momentum dependences can provide access to a very rich QCD phenomenology provided that enough experimental information is recorded. For polarisation-dependent terms of the cross-section as the one in Eq. 2, a common practice adopted by experiments is to measure the so-called spin asymmetry

$$A_{UT} = \frac{\sigma_{UT}}{\sigma_{UU}} = \frac{1}{f S_T} \frac{N^\uparrow - N^\downarrow}{N^\uparrow + N^\downarrow}, \quad (4)$$

where S_T is the polarisation degree and f the dilution due to any not-polarisable component of the target, and $N^{\uparrow,\downarrow}$ is the extracted number of $ep^{\uparrow,\downarrow} \rightarrow e'hX$ events for positive (\uparrow) or negative (\downarrow) target polarisations. The advantage is to get a robust observable where most of the systematics due to instrumental artefacts cancel at first order. The disadvantage is that any structure function analysis based on the Fourier decomposition of the asymmetry should disentangle the wanted azimuthal modulations at numerator with the ones of the polarisation-independent cross-section σ_{UU} at the denominator, as will be discussed in Section 4. Provided that the unpolarised cross-section is known with enough precision, the asymmetry amplitude can be related to the structure function ratio and used to extract direct information on the parton distributions:

$$A_{UT}^{\sin(\phi+\phi_S)} = \frac{F_{UT}^{\sin(\phi+\phi_S)}}{F_{UU}} = \frac{C [wh_1 H_1^\perp]}{C [f_1 D_1]}. \quad (5)$$

Some of the cross-section terms in Eq. 1, for example the azimuthal modulations in the unpolarized case or involving longitudinally-polarized beam and unpolarized target, gets contributions only at subleading level and suppressed by powers of the hard scale Q (higher-twist). This contributions are interesting as correlated to the quark-gluon correlations, and can be interpreted as due to the color-Lorentz forces experienced by a quark in the surrounding gluon medium.

The full mapping of TMDs requires measurements with good detector acceptance over the azimuthal angle ϕ and ϕ_S around the virtual photon direction, covering large kinematic ranges in x , z , P_{hT} and Q^2 , hadron identification for *flavour tagging*, and the use of polarised beam and targets.

Target spin asymmetries have been published by the HERMES Collaboration on the proton [22–24] and the COMPASS collaboration on deuterium and proton targets [25, 26], for the first time directly indicated significant azimuthal moments generated both by the Collins and the Sivers effects. These asymmetries become larger with increasing x , indicating that spin-orbit correlations are more relevant in the kinematic region where valence quarks have visible presence. Measurements of SSAs at JLab, performed with longitudinally polarised NH_3 [27] and transversely polarised ^3He [28–31] indicate that spin orbit correlations may be significant for certain combinations of spins of quarks and nucleons and transverse momentum of scattered quarks. Large spin-azimuthal asymmetries have been observed at JLab for a longitudinally polarised beam [32] and a transversely polarised ^3He target [33], consistent with corresponding measurements at HERMES [34] and COMPASS [35], which have been interpreted in terms of higher-twist contributions, related to quark-gluon correlations.

There have been many interesting model studies, see for example [13, 36–40]. These models and their calculations could play a very important role as a first step to describe the experimental observations, to give an intuitive way to connect the physical observables to the par-

tonic dynamics, and to provide key inputs to unravel the partonic structure of the nucleon. This will help us to address fundamental questions, such as how the quark spin and its orbital angular momentum contribute to the nucleon spin. In addition, very exciting results of TMDs have come from recent lattice QCD calculations [41–43], indicating that spin-orbit correlations could change the transverse momentum distributions of partons.

3.1 Measuring TMDs: unpolarised quark distributions

Hadron multiplicities in SIDIS reactions have since long time been used to study quark fragmentation, complementing the measurements done at higher energies at the e^+e^- collider machines [1]. Noteworthy, SIDIS measurements with various targets and hadron identification capability allow the study of fragmentation functions with enhanced flavour sensitivity.

The hadron multiplicities study is now being extended to a multi-dimensional analysis, in particular looking to the transverse momentum dependence and its correlations with other kinematic variables. From the observed transverse hadron momentum P_{hT} , information can be gathered on the intrinsic k_\perp and the p_\perp generated during fragmentation by unfolding Eq. 6. Up to order k_\perp/Q , momentum conservation gives $\mathbf{P}_{hT} = z\mathbf{k}_\perp + \mathbf{p}_\perp$ and the structure function F_{UU} is given by the convolution integral $C[fD]$, or:

$$F_{UU}(P_{hT}) = x \sum_q e_q^2 \int \delta^2(\mathbf{p}_\perp - z\mathbf{k}_\perp - \mathbf{P}_{hT}) f(x, k_\perp) D(z, p_\perp) d\mathbf{p}_\perp^2 d\mathbf{k}_\perp^2 \quad (6)$$

For example, a common assumption is the Gaussian ansatz for the transverse momentum dependence of distribution and fragmentation functions with the average P_{hT} by

$$\langle P_{hT}(z) \rangle = \frac{\sqrt{\pi}}{2} \sqrt{z^2 \langle k_\perp^2 \rangle + \langle p_\perp^2 \rangle}. \quad (7)$$

The transverse momentum dependence may be different for the different flavours. Calculations of transverse momentum dependence of TMDs in different models [40, 44–46] and on lattice [41, 43] indicate that the dependence of the transverse momentum distributions on the quark polarisation and flavour may be significant. For example it is found, somewhat unexpectedly, that the average transverse momentum square of antiquarks is considerably larger than that of quarks [47] which has later been linked to a more general consequence of the dynamical chiral-symmetry breaking [48]. In the fragmentation process, one would expect that the *dis-favoured* fragmentation of a quark into a hadron with different valence quarks be more involved and thus with a broader transverse momentum spectrum with respect the *favoured* fragmentation of a quark into a hadron with same valence quark. Moreover, the frequently used assumption of factorisation in x and k_\perp (or z and p_\perp) may be significantly violated, i.e. the predicted average transverse momentum square $\langle k_\perp^2 \rangle$ of

quarks and antiquarks depends strongly on their longitudinal momentum fraction x within the framework of the chiral quark soliton model.

Semi-inclusive electro-production of charged pions has been measured from both proton and deuteron targets, using a 5.5 GeV energy electron beam in Hall-C at Jefferson Lab [49]. In the limited $P_{hT}^2 < 0.2$ explored, the P_{hT} dependence from the deuteron was found to be slightly weaker than from the proton. In the context of a simple model this would suggest that transverse momentum distributions may depend on the flavour of quarks.

Recently, multiplicities of charged pion and kaon mesons have been measured by HERMES using the electron beam scattering off hydrogen and deuterium targets [50]. In addition, multiplicities of charged hadrons produced in deep inelastic muon scattering off a ${}^6\text{LiD}$ target have been measured at COMPASS [51]. These high-statistics data samples have been used in phenomenological analyses to extract information on the flavour dependence of unpolarised TMD distribution and fragmentation functions. Restricting the ranges of the available data to $Q^2 > 1.69$ (GeV/c) 2 , $z < 0.7$ and $0.2 \text{ GeV}/c < P_{hT} < 0.9 \text{ GeV}/c$, the authors of Ref. [52] were able to obtain a reasonable description of the experimental data with a TMD Gaussian model with flavour independent and constant widths, $\langle k_{\perp}^2 \rangle$ and $\langle p_{\perp}^2 \rangle$. Nevertheless, indications were reported that favoured fragmentation functions into pions have smaller average transverse momentum than unfavoured fragmentation functions and fragmentation functions into kaons [53], consistent with predictions based on the NJL-jet model [54].

A precise determination of the separate values of $\langle k_{\perp}^2 \rangle$ and $\langle p_{\perp}^2 \rangle$ would require the simultaneous analysis of other observables, like the azimuthal dependencies of the SIDIS cross-section discussed in Section 3.5, which are sensitive to the ratio $\langle k_{\perp}^2 \rangle / \langle p_{\perp}^2 \rangle$. An important complementary information should come from the extension of the fragmentation studies done at the e^+e^- collider machines to the transverse momentum dependence. Measurements of inclusive differential cross sections for charged pion and kaon production in e^+e^- annihilation, carried out at a centre-of-mass energy of $\sqrt{s} = 10.52 \text{ GeV}$ and unprecedented luminosity, have recently shown the potentiality of the B-factories [55, 56].

COMPASS is finalising the analysis of the hadron multiplicities from the 2006 ${}^6\text{LiD}$ data [57], covering a broader P_{hT} range and showing the need to introduce more complex curves than a single Gaussian to fit the data (see Fig. 3) and will collect soon data on a liquid hydrogen target as described in the approved phase-II proposal [58]. A broad program of measurements is planned in different experimental halls of JLab after the beam energy and detector upgrades. Among the various planned experiments, there are some dedicated to precise measurements of the SIDIS cross sections for charged pions and kaons at low P_{hT} from hydrogen and deuterium targets [59], that can be used to extract the mean transverse momentum of up and down quarks in the nucleon. Extended exploration from current to target fragmentation region [60] are also planned, with the measurements of the x , z and P_{hT} de-

pendences of different azimuthal moments for pions and kaons in the valence region.

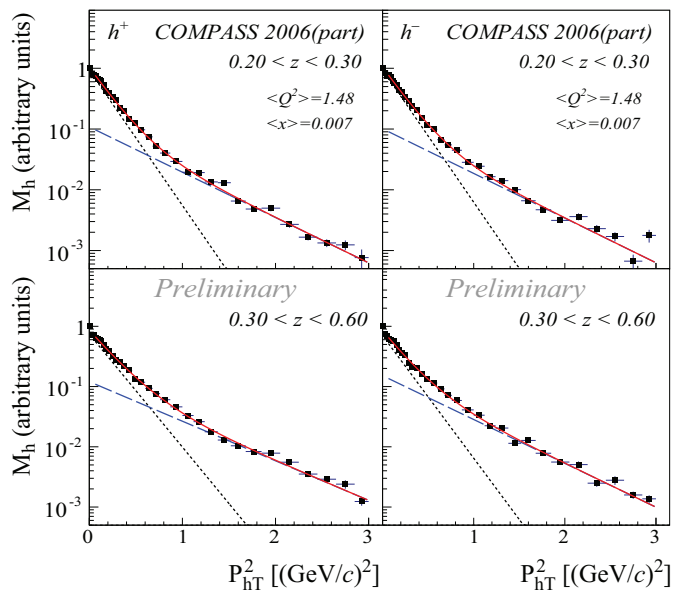


Fig. 3. Examples of positive and negative hadron multiplicities (scaled to arbitrary units) with 1-exponential (dotted line) and 2-exponentials (dashed line) fits from COMPASS [57].

A complete comprehension would require the study of longitudinal to transverse virtual-photon absorption SIDIS cross section ratio $R = \sigma_L / \sigma_T$. Although R appears in the denominator of all the azimuthal asymmetries related to the TMDs investigation, it is up to date unknown. The phenomenological analyses have typically assumed either zero or the values determined from inclusive DIS. The precise measurement of R for charged pions and kaons [61], and neutral pions, will help to shed light on the nature of the SIDIS reaction mechanism, in particular regarding the higher-twists contributions, which could be particularly important at the rather modest energies of JLab.

As highlighted by phenomenological analyses relating results of different reaction channels [36], the TMD distribution widths change with the centre-of-mass energy. This is connected with the non-trivial evolution properties of the TMD functions, now at the centre of a strong activity [62–64]. The novel high-precision SIDIS measurements, in conjunction with e^+e^- annihilation and Drell-Yan data, will be crucial to validate the TMD evolution formalism under development.

3.1.1 Medium modifications

The detailed understanding of the properties of hot and cold nuclear matter is one of the topical problems of QCD. When a hard parton passes through a medium, either cold nuclear matter or quark-gluon plasma, it loses energy due to multiple scattering and induced gluon bremsstrahlung. Initial/final state multiple parton re-scattering

in a large nucleus plays an important role in revealing the properties of cold nuclear matter and much efforts have been devoted to the study of transverse momentum broadening in eA and pA collisions. For example, the quark fragmentation function into final hadrons in a nuclear medium will be modified as compared to that in vacuum. The modification in general involves suppression of leading hadrons in deeply inelastic scattering off nuclei or high-transverse-momentum hadron in high-energy heavy-ion collisions, a phenomena referred to as jet quenching. As a consequence, measurements of modification of the observed hadron spectra in medium allow to extract information on medium properties. There is therefore a growing interest in the study of nuclear dependence of the TMD parton distribution functions [65]. Within the TMD factorisation approach [20,21], the non-trivial gauge link appearing in the matrix element definition for nuclear TMDs becomes the main source of leading nuclear effects [65,66].

The hadronisation process in free space has been studied extensively in e^+e^- annihilation experiments [67–69]. As a result the spectra of particles produced and their kinematic dependencies are rather well known. However, little is known about the space-time evolution of the process. Semi-inclusive production of hadrons in deep-inelastic scattering of leptons from atomic nuclei provides a way to investigate this space-time development: electro-production of hadrons has the virtue that the energy and the momentum of the struck parton are well determined, as they are tagged by the scattered lepton. By using nuclei of increasing size one can investigate the time development of hadronisation.

A series of semi-inclusive deep-inelastic scattering measurements on helium, neon, krypton, and xenon targets has been performed at HERMES to be compared with a deuteron target in order to study hadronisation [70]. A multi-dimensional analysis has been performed to help disentangling the various kinematic dependencies [71]. The HERMES SIDIS data have been used to study medium properties such as the jet transport parameter \hat{q} , the average squared transverse momentum broadening per unit length, which can be related in a model dependent way to the gluon distribution density [72]. From a fit of the HERMES data a value of $\hat{q} \equiv 0.020 \pm 0.005 \text{ GeV}^2/\text{fm}$ at the centre of a large nucleus has been extracted. The resulting \hat{q} from SIDIS data can be compared to the higher ones derived from the suppression of large p_\perp single inclusive hadrons in heavy-ion collisions. Model-dependent values for the jet transport parameter \hat{q} at the centre of the most central heavy-ion collisions have been extracted by a phenomenological study [73] of experimental data from both RHIC [74,75] and LHC [76,77]. For a quark with initial energy of 10 GeV and at an initial time $\tau_0 = 0.6 \text{ fm}/c$, $\hat{q} \equiv 1.2 \pm 0.3 \text{ GeV}^2/\text{fm}$ in Au+Au collisions at $\sqrt{s} = 200 \text{ GeV}/n$ and $\hat{q} \equiv 1.9 \pm 0.7 \text{ GeV}^2/\text{fm}$ in Pb+Pb collisions at $\sqrt{s} = 2.76 \text{ TeV}/n$.

A complementary approach is to measure the broadening of the transverse momentum distribution of various hadrons in SIDIS. This observable should be mostly sensitive to the partonic stage of hadron production as trans-

verse momentum broadening ceases at the point of colour neutralisation. Measurements were done for π^+ at a beam energy of 6 GeV by the CLAS experiment as a function of ν , Q^2 , and z with carbon, iron and lead targets [78]. For the heaviest target a hint of a saturation behaviour was found. This would be expected in the case that the quark evolves into a pre-hadron within the medium for the largest nucleus. At the higher 27 GeV beam energies of HERMES [79], there is no clear indication of such a saturation at large atomic mass numbers. This behaviour suggests that the colour neutralisation happens near the surface of the nucleus or outside at the average HERMES kinematics. In this case the broadening is expected to be simply proportional to the medium thickness, i.e. proportional to the mass number to the 1/3 power.

The above results on jet transport parameter and p_\perp -broadening has been used to get numerical estimates of the suppression of azimuthal asymmetries in SIDIS off unpolarised and polarised nuclear targets using the TMDs formalism [80,81]. The experimental investigation of medium modification of quark fragmentation and spin-orbit correlation will be extensively pursued at the upgraded Jefferson Lab facility, for which several related experimental proposal already exist [82,83].

3.1.2 Low- x physics

In the region of very low values of x , where transverse-momentum ordering does not apply, fixed-order perturbative approaches are theoretically disfavoured and cannot be expected to describe the physics of the scaling violation. In that kinematic region specific factorisation schemes [84,85] have been introduced that naturally incorporate transverse-momentum unintegrated (TMD) parton distributions. Such schemes have been used to perform fits to the HERA measurements of the F_2 structure function [86], in the range $x < 0.005$, $Q^2 > 5 \text{ GeV}^2$, and to measurements of the charm F_2^{charm} structure function [87], in the range $Q^2 > 2.5 \text{ GeV}^2$, in order to make a determination of the TMD gluon density including also the valence quark contribution [88]. The extracted TMD gluon distributions can be used to make predictions for hadron-hadron collider processes, i.e. W -boson Drell-Yan production [89]. The comparison with LHC data on W -boson production associated with jets [90,91] shows a reasonable agreement both for the jet transverse momentum distribution and angular correlations. However, a still significant uncertainty is derived from the extracted TMD parton distributions as the computed p-p cross sections are not dominated by very small values of x . It is conceivable that combining p-p measurements on vector boson production with the DIS measurements may help to constrain TMD PDFs in a broad range of x . Thanks to its high luminosity and the feasibility for an energy scan, an EIC would be particularly sensitive to the gluon distribution and QCD dynamics at small x and therefore a promising candidate to validate generalised evolution schemes matching the low and moderate x regimes [92] and complement the studies above with the investigation

of the transition to the high parton density regime, i.e., the phenomenon of saturation [93].

3.2 Measuring TMDs: helicity distributions

The longitudinal spin structure of the nucleon has been investigated over the past two decades by the SMC [94], E142 [95], E143 [96], HERMES [97], JLab [98–100] and COMPASS [101–103] Collaborations. The main focus of those experiments, measuring inclusive and semi-inclusive DIS, were x -dependences of virtual photon asymmetry, A_1 , to determine the contributions of quark spins to the spin of nucleons as well as the spin quark distribution functions for valence and sea quarks.

HERMES [34], COMPASS [104] and CLAS [27] have measured azimuthal asymmetries in semi-inclusive production of positive and negative hadrons on longitudinally polarised targets finding non-zero contribution for few of the possible modulations, but with relatively large statistical errors given the smallness of the expected effects. The $\sin\phi$ modulation amplitudes (Fig. 4) are given by a combined effect from the twist-3 PDFs h_L and f_L^\perp to $d\sigma_{UL}$ as well as from the twist-2 transversity PDF h_1 and Sivers PDF f_{1T}^\perp in $d\sigma_{UT}$, all scaled by factor Mx/Q . The individual PDF contributions can not be separated within a single experiment. The observed x dependence of this amplitude is less pronounced in COMPASS [104] than in HERMES [105] due to difference in selection and kinematic coverage, but come in agreement when the same analysis is applied.

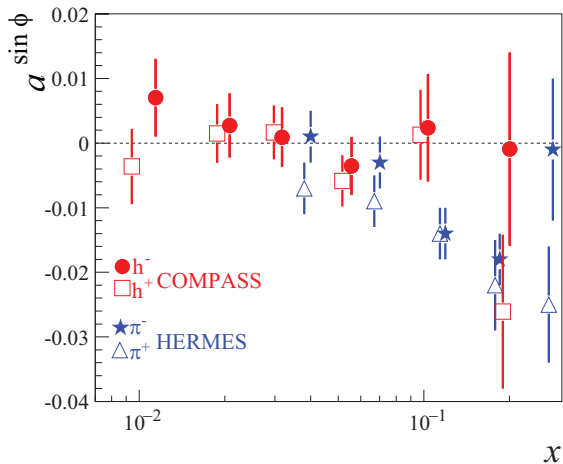


Fig. 4. Dependence of the modulation amplitude $a^{\sin\phi}$ on x from COMPASS [104] for charged hadrons and HERMES [105] for identified pions.

Wide acceptance in P_{hT} in SIDIS measurements in addition would allow for studies of transverse momentum dependence of different distribution and fragmentation functions as well as transition from TMD regime to perturbative regime. Kinematic dependencies of single and double spin asymmetries have been measured in a wide range in x

and P_{hT} with CLAS using a longitudinally polarised proton target. Significant single-spin asymmetries have been observed in semi-inclusive pion electro-production. Measurements of the P_{hT} -dependence of the double spin asymmetry, performed for the first time, indicate the possibility of different average transverse momenta for quarks aligned or anti-aligned with the nucleon spin [27].

Precision measurements using the upgraded CLAS detector (CLAS12) with polarised NH_3 and ND_3 targets will allow access to the k_\perp -distributions of u and d -quarks aligned and anti-aligned with the spin of the nucleon. Projections for the resulting P_{hT} -dependence of the double spin asymmetries for all three pions are shown in Fig. 5 for an NH_3 target [106, 107]. Integrated over transverse momentum, the data will also be used to extract the k_\perp -integrated standard PDFs.

Measurements of spin asymmetries as a function of the final hadron transverse momentum at Electron Ion Collider [108] (EIC) will extend (see Fig. 5 and 6) measurements at JLAB12 [106, 109] to significantly higher P_{hT} and Q^2 allowing comparison with calculations performed in the perturbative limit [110]. Extending measurements of P_{hT} -dependent observables to significantly lower x will provide access to transverse momentum dependence of quarks beyond the valence region.

Much higher Q^2 range accessible at EIC would allow for studies of Q^2 -dependence of different higher-twist SSAs, which, apart from providing important information on quark-gluon correlations are needed for understanding of possible corrections from higher-twists to leading-twist observables.

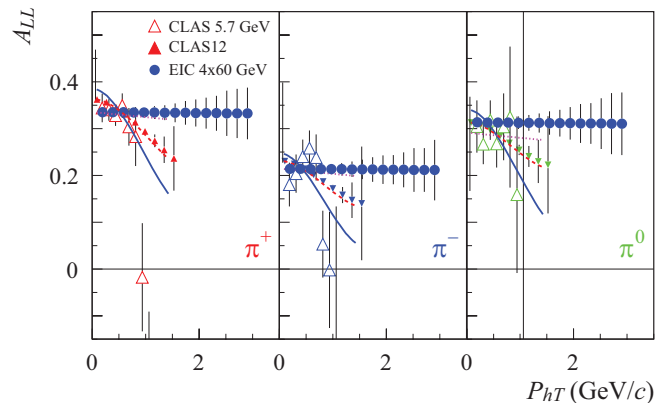


Fig. 5. Double-spin asymmetry, A_{LL} , for pion production, using the EIC [111] configuration with 4 GeV electrons and 60 GeV protons (100 days at $10^{34} \text{ cm}^{-2} \text{ sec}^{-1}$), as a function of P_{hT} , compared to published data from CLAS [27] and projected CLAS12 measurements [107].

3.3 Measuring TMDs: transversity

The transversity distribution [4, 113] and its first moment, the tensor charge, are as fundamental for understanding

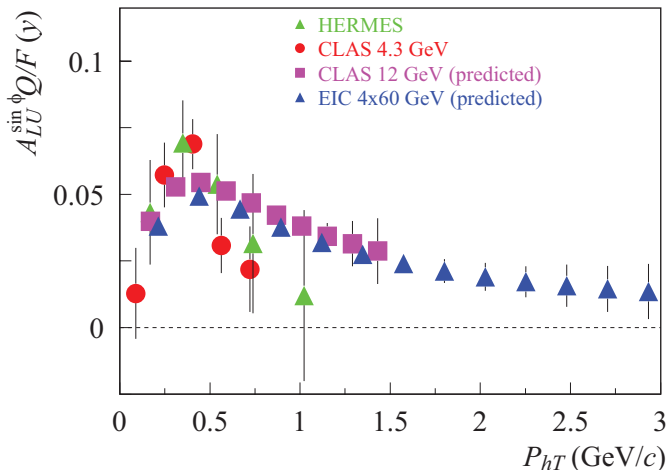


Fig. 6. Projections for the same EIC running conditions of Fig.5 for the higher-twist lepton spin asymmetry, compared to published data from CLAS [32] and HERMES [112], and projected CLAS12 [106] data in one x, z bin ($0.2 < x < 0.3$, $0.5 < z < 0.55$).

of the spin structure of the nucleon as are the helicity distribution g_1 and the axial vector charge. Differently from g_1 , h_1 is chirally odd, i.e. requires a quark helicity flip that cannot be achieved in inclusive DIS. For non-relativistic quarks h_1 is equal to the helicity distribution g_1 , thus any differences among the two functions probes the relativistic nature of quarks. The h_1 function has a very different Q^2 evolution than g_1 since there is no gluon transversity in the nucleon. The tensor charge is reliably calculable in lattice QCD with $\delta\Sigma = \sum_f \int_0^1 dx (h_1^f - \bar{h}_1^f) = 0.562 \pm 0.088$ at $Q^2=2$ GeV², which is twice as large as the value of the axial charge [114]. A similar quantity ($\delta\Sigma \approx 0.6$) was obtained in the effective chiral-quark-soliton model [115].

3.3.1 The Collins asymmetry

The main source of information on the transversity PDFs is at present the Collins asymmetry, which couples h_1 to the Collins fragmentation function H_1^\perp :

$$A_{UT}^{\sin(\phi_h + \phi_s)}(x) \simeq \frac{\sum_q e_q^2 h_1^q(x) \otimes H_1^{\perp, q \rightarrow h}}{\sum_q e_q^2 f_1^q(x) \otimes D_1^{q \rightarrow h}}$$

where \otimes indicate the convolution integrals between the quark transverse momentum and the transverse momentum acquired by the hadron in the fragmentation process with respect to the quark. In this case the asymmetry as a function of x is obtained by integrating over the other kinematic variables such as z , P_{hT} and Q^2 .

The Collins asymmetry has been measured by COMPASS on deuterons (⁶LiD) and on protons (NH₃) for unidentified hadrons (dominated by pions), π and K (Fig. 7), by HERMES on protons, for π and K (Fig. 8) and by Hall A on neutrons (³He) for π and K (Fig. 9).

Both in COMPASS and in HERMES (when the same sign convention is adopted ¹), the Collins asymmetries measured for charged π on protons show a clear negative signal for π^+ and a positive signal for π^- as a function of x , z and P_{hT} . The asymmetries measured by COMPASS and HERMES have the same amplitude once the HERMES data are corrected for the depolarisation factor, giving important information on the kinematic dependencies of the transversity PDF and Collins FF. The trend is confirmed for K^+ , while K^- and K^0 signals are smaller (or absent), and more statistics is needed. A significant asymmetry was measured recently by Belle [116–118] and BaBar [119, 120] experiments, indicating that the Collins function H_1^\perp is indeed large. The SIDIS result is an indication that favoured and un-favoured Collins fragmentation functions are opposite but of similar magnitude, an observation compatible with the measurements done at e^+e^- machines [116–118]. The null COMPASS results on deuteron allows to constrain h_1^d .

A global analysis of COMPASS, HERMES and Belle data allowed a first extractions of transversity PDFs and Collins FFs [121, 122], showing that transversity function is sizable and different from zero, with opposite sign and similar amplitude for both the u and d quark, while at the same time favoured and unfavoured Collins FF are also large, with similar amplitude but opposite sign. The Collins asymmetries on n from Hall A, are compatible with zero as expected from the fits of proton and deuteron data.

3.3.2 The two-hadron asymmetry

The transverse spin asymmetry in the distribution of the azimuthal plane of hadron pairs in the current jet of DIS have been measured by HERMES with the proton target and by COMPASS both with the deuteron and the proton targets. Also for this asymmetry there are some small differences between the analysis performed by the two experiments, that comprises a different definition of transverse vector of the two hadrons (the azimuthal angle derived in the two cases eventually coincide in the γ^*N system). Apart from slightly different DIS cuts, HERMES requires a missing mass larger than 2 GeV/ c^2 to avoid contributions from exclusive two-pion production. Also a minimum pion momentum of 1 GeV is required for pion identification. In the COMPASS analysis, the event selection is more similar to that of the single hadron asymmetries, with a decreased minimum z energy fraction required for both the hadrons $z_{1,2} > 0.1$ and an upper limit of 0.9. In the extraction of the asymmetries no dependence on the $\sin\theta$ component of the dihadron fragmentation function is taken into account since in the COMPASS kinematics the $\sin\theta$ distribution is strongly peaked at one ($\langle \sin\theta \rangle = 0.94$) and the $\cos\theta$ distribution is symmetric around zero. The larger W accessible in COMPASS as compared to HERMES and JLab resulted in a higher sample of multi-hadron events and consequently more precise

¹ The COMPASS convention is adopted for the following discussion.

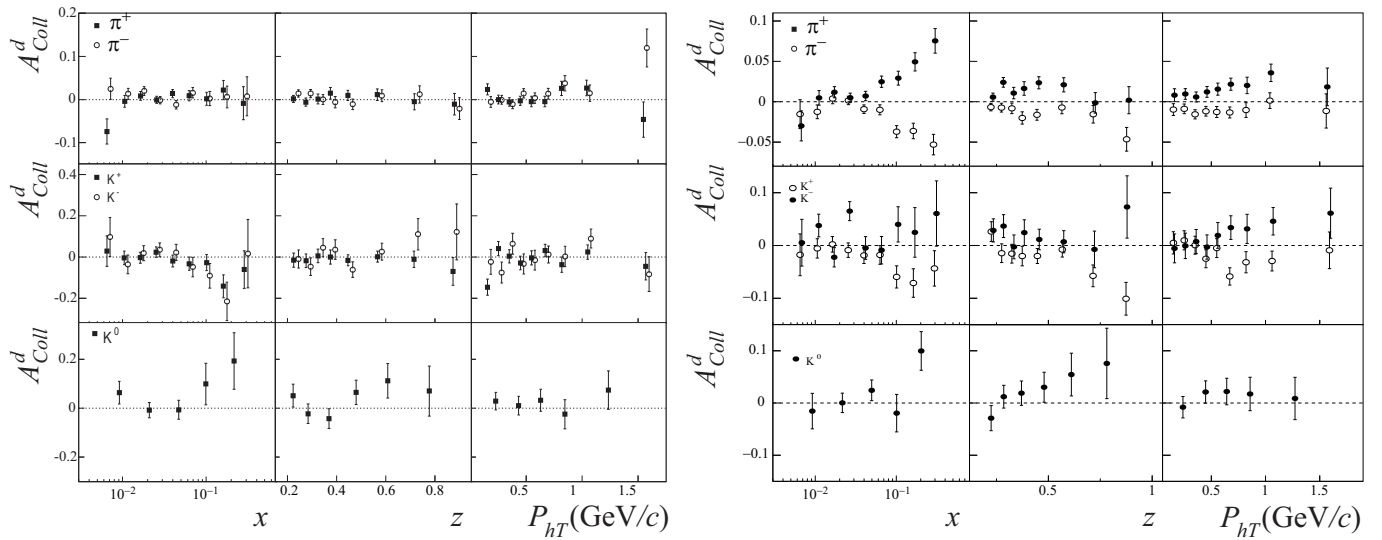


Fig. 7. COMPASS measurements of the Collins asymmetries for π^\pm and $K^{\pm,0}$ on deuterons (left) and protons (right).

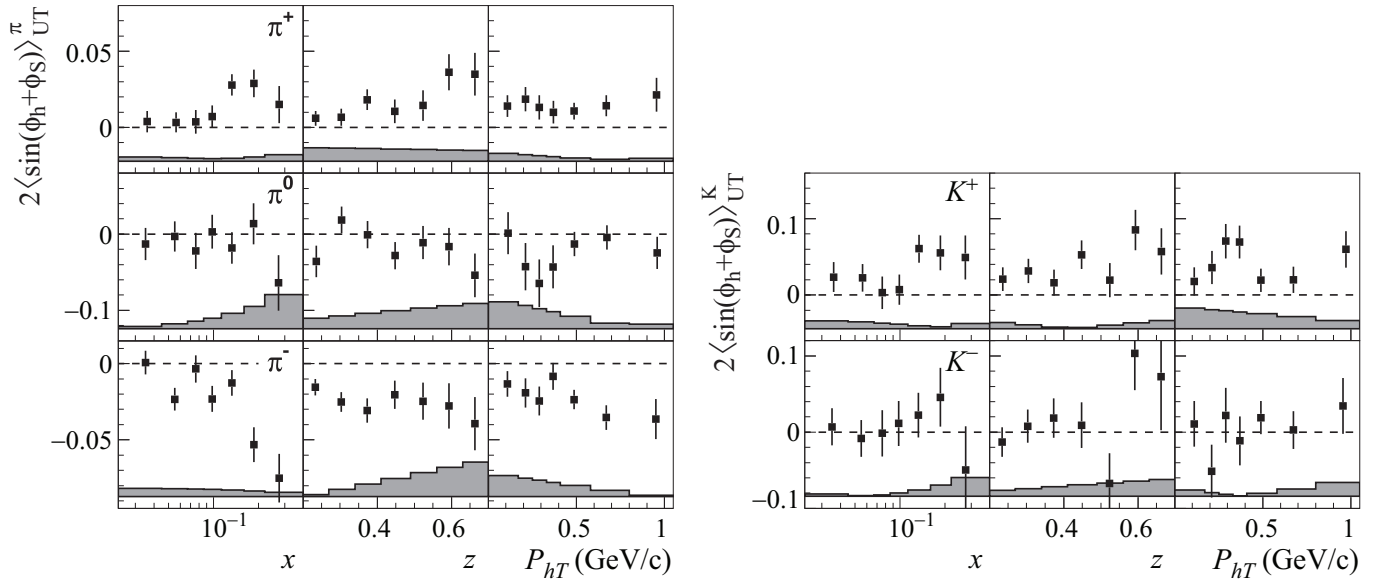


Fig. 8. HERMES measurements of the Collins asymmetries on protons for π^\pm (left) and K^\pm (right).

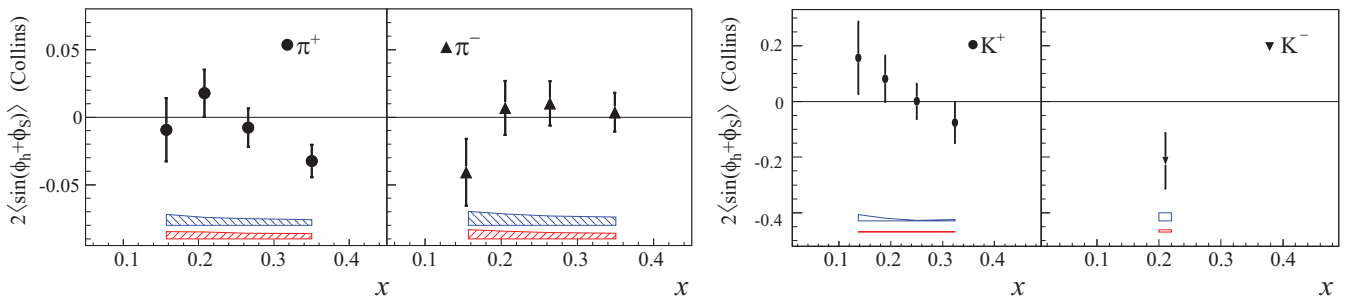


Fig. 9. Hall A measurements of the Collins asymmetries on neutrons for π^\pm (left) and K^\pm (right).

$2h$ asymmetries. COMPASS results are shown in Fig. 10 for both protons and deuteron and for different particles combinations. A clear signal in the valence region is only visible for $\pi^+\pi^-$ combination.

Recently COMPASS pointed out that the dihadron asymmetry as functions of x and the Collins asymmetries for both π^+ and π^- show important similarities, i.e the dihadron asymmetry is slightly larger in magnitude, but very close to the values of the Collins asymmetry for positive hadrons and to the value of the negative pions, after reversing the sign of the asymmetry. Taking into account correlations between azimuthal angles of positive and negative pions in the two hadron sample, suggesting that in the multi-hadrons fragmentation of the struck quark azimuthal angles of positive and negative hadrons created in the event differ preferably by $\approx \pi$, this strongly hints for a common origin for the Collins mechanism and the dihadron fragmentation function, as originally pointed out by the 3P_0 Lund model [123], or by the recursive string fragmentation model [124].

3.4 Measuring TMDs: the Siverson distribution

Among the off-diagonal elements, the Siverson f_{1T}^\perp and the Boer-Mulders h_{1T}^\perp functions are of particular interest.

The Siverson function describes the difference between the probability to find a quark with light-cone momentum fraction x and transverse momentum k_\perp inside a hadron polarised transversely to its momentum direction, and the one where the polarisation points in the opposite direction. The Siverson function has been phenomenologically extracted by several groups, mainly from analysing the azimuthal distribution of a single hadron in SIDIS [125–128].

The probability of finding an unpolarised quark with longitudinal momentum fraction x and transverse momentum k_\perp inside a transversely polarised target is given by:

$$\Phi^q(x, k_\perp; S) = f_1^q(x, k_\perp^2) - \frac{(\hat{P} \times k_\perp) \cdot S_T}{M} f_{1T}^{\perp q}(x, k_\perp^2). \quad (8)$$

The Siverson contribution to the $F_{UT}^{\sin(\phi-\phi_S)}$ structure function, being leading-twist, is expected to survive at higher Q^2 . Recently the Siverson asymmetry has been calculated and compared at different scales using the TMD evolution equations applied to previously existing extractions [64].

As for the Collins asymmetry, the Siverson asymmetry has been measured by COMPASS on deuterons (${}^6\text{LiD}$, Ref. [101]) and on protons (NH_3 , Ref. [129]) for unidentified hadrons (dominated by pions), π and K (Fig. 11, Refs. [130] and [131]), by HERMES on protons, for π and K (Fig. 12, Ref. [23]) and by Hall A on neutrons (${}^3\text{He}$) for π (Fig. 13, Ref. [28]).

For both COMPASS and HERMES the proton asymmetries for negative pions and kaons, as well as for neutral kaons are compatible with zero, while for positive pions and kaons there is a clear evidence for a positive signal. For COMPASS the signal extends over the full measured x region and increases with z . As for HERMES, the K^+ signal is larger than the π^+ one, which

indicates a possibly not negligible role of sea quarks. Unlike the case of the Collins asymmetry, the Siverson asymmetry measured by COMPASS at large x for positive pions and kaons is smaller than the one from HERMES, indicating a non-trivial dependence on Q^2 [64]. Several fits, which include the recently revisited Q^2 evolution, were performed using HERMES asymmetries, COMPASS asymmetries on deuteron and for unidentified hadrons on proton, and JLab Hall A asymmetries on ${}^3\text{He}$. Some of these fits [19, 132, 133], which employ TMD evolutions, are shown to well reproduce the results of the three experiments, and account therefore for the observed discrepancies between HERMES [23] and COMPASS [129] data. An example from Ref. [64] is shown in Fig. 14, where predictions have been made for the non-trivial behaviour of the Siverson asymmetry as a function of Q^2 .

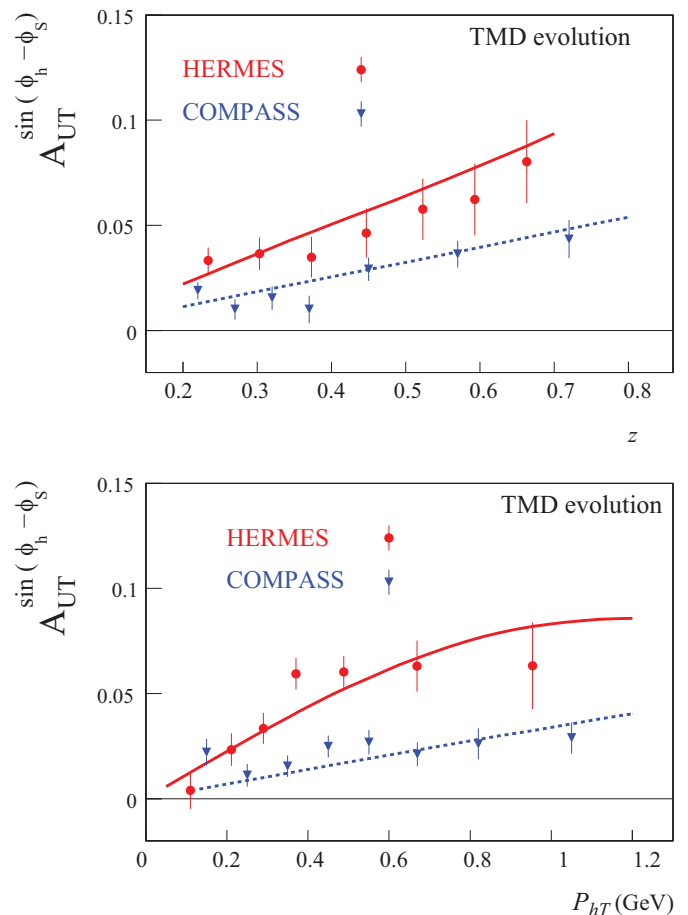


Fig. 14. HERMES [23] and COMPASS [129] Siverson asymmetries. The solid line is the result of the fit from Ref. [128] of HERMES data. The dashed curve is the result of evolving to the COMPASS scale using the full TMD-evolution of Ref. [134] obtained by [64].

COMPASS has very recently measured the Siverson asymmetry for gluons [135] from the data collected with the ${}^6\text{LiD}$ and NH_3 transversely polarised targets. The Siverson

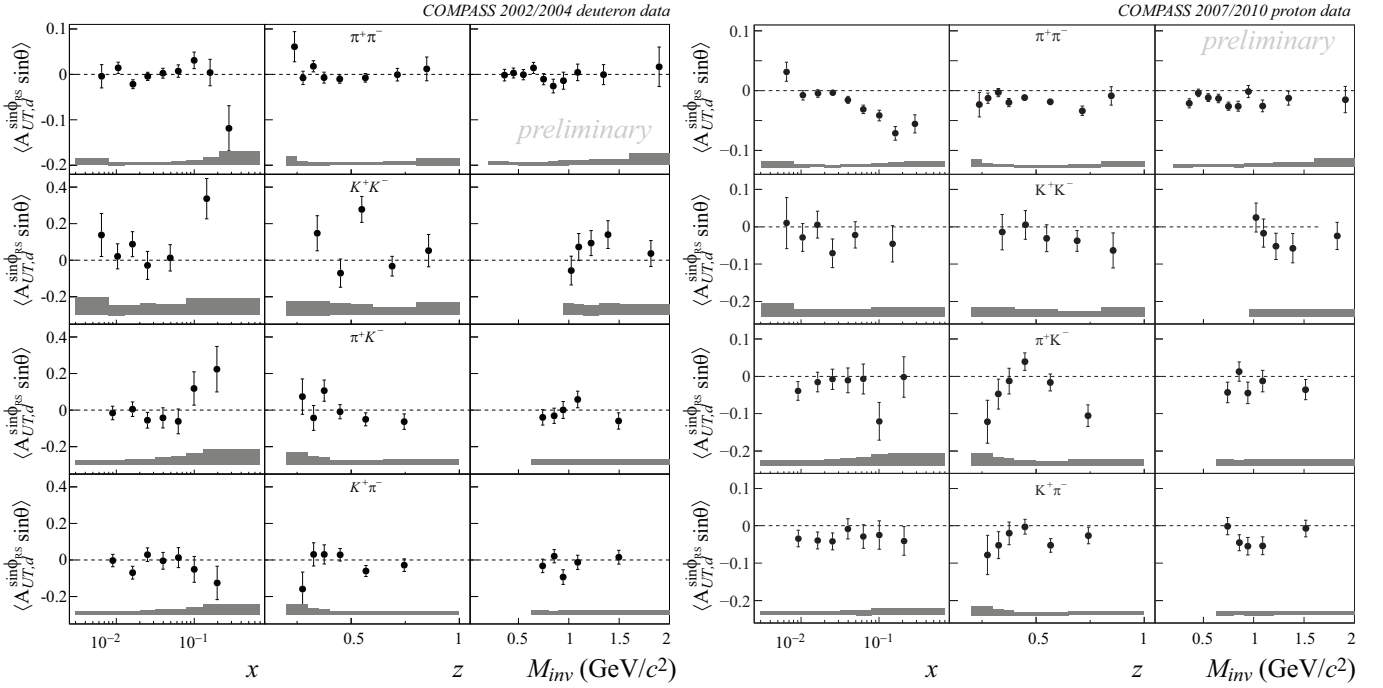


Fig. 10. COMPASS measurements of the two identified hadron asymmetries of $\pi^+\pi^-$, π^+K^- , $K^+\pi^-$ and K^+K^- on deuterons (left) and protons (right).

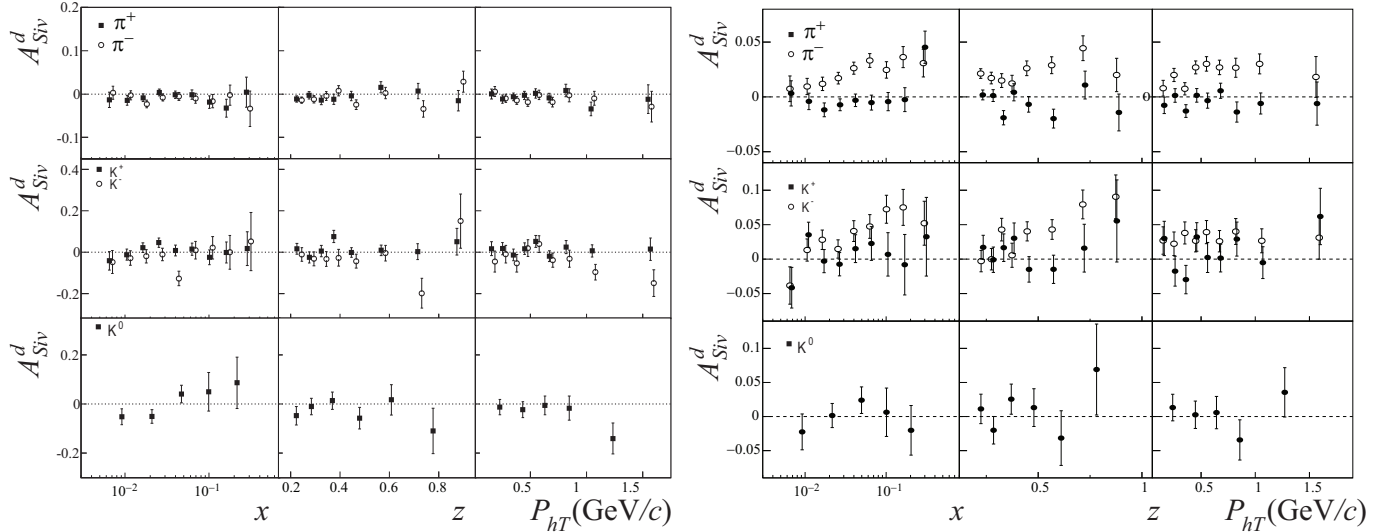


Fig. 11. COMPASS measurements of the Sivers asymmetries for π^\pm and $K^{\pm,0}$ on deuterons [130] (left) and protons [131] (right).

gluon asymmetry was extracted using a technique similar to the one adopted for the gluon helicity Δg analysis [136, 137]. On ${}^6\text{LiD}$ the asymmetry is small (Fig. 15, top) and compatible with zero, within the present experimental precision, as was expected from phenomenological studies of existing data [138, 139]. But the higher precision of the proton data is surprisingly showing a negative asymmetry for the gluon Sivers; a quite interesting and unexpected result.

The test of the sign change of the Sivers function from SIDIS to Drell-Yan:

$$(f_{1T}^\perp)_{\text{SIDIS}} = - (f_{1T}^\perp)_{\text{DY}} \quad (9)$$

is a critical test of the TMD factorisation. This test is presently undergoing in COMPASS, that is collecting in 2015 the first ever polarised Drell-Yan data with 190 GeV π^- impinging on a transversely polarised proton target. For a direct comparison with the SIDIS data the relative large SIDIS statistics collected by COMPASS allowed to measure the behaviour of the asymmetries as a function

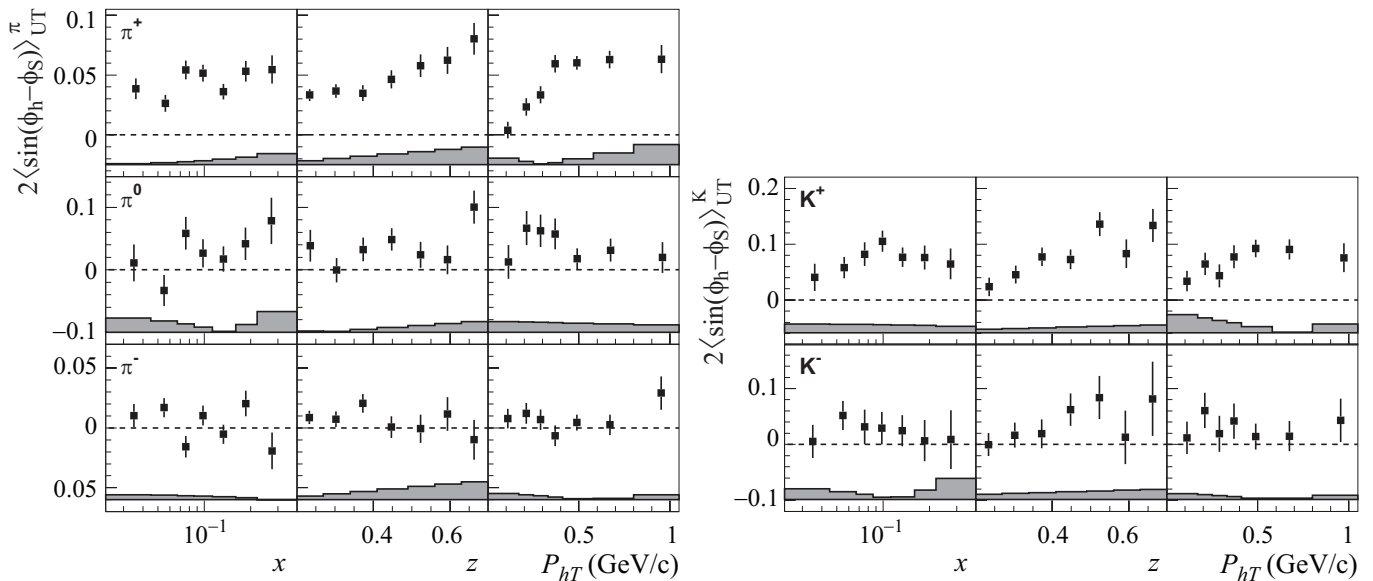


Fig. 12. HERMES measurements of the Sivers asymmetries on protons [23] for π^\pm (left) and K^\pm (right).

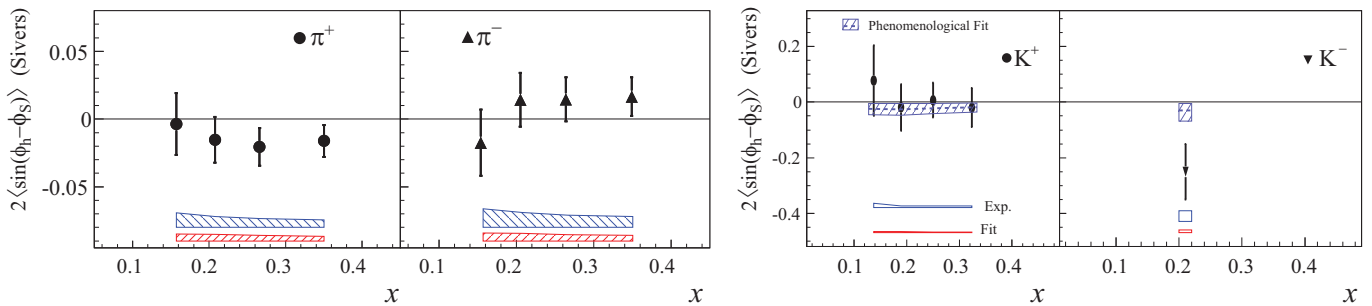


Fig. 13. Hall A measurements of the Sivers asymmetries on neutrons [28] for π^\pm (left) and K^\pm (right).

of Q^2 , needed since Drell-Yan $\mu\mu$ events are selected by cutting in the invariant mass spectrum $M_{\mu\mu}$ in the region above the J/ψ resonance, i.e. $M_{\mu\mu} > 4 \text{ GeV}/c^2$ (or $Q^2 > 16 \text{ GeV}^2/c^2$). The Collins and Sivers asymmetries as a function of x for different values of Q^2 are shown in Fig. 16. Non-zero effects were detected for asymmetries in all ranges. A clear signal is visible for Sivers with positive hadrons in all ranges and some hints of possible non-zero effect can be noticed for negative hadrons at relatively large x - Q^2 . The Collins asymmetry is visible both for positive and negative hadrons in all Q^2 -ranges except in the very low- x region.

Several other Drell-Yan proposals were approved to measure TMDs [140,141] and perform that test [142]. The possibility of a node in the x -dependence of the Sivers function has been discussed in light of this important test [143]. As the Sivers function describes a difference of probabilities it is not necessarily positive definite.

A recent extraction of the Sivers function for u , d , and s flavours, also based on the SIDIS results from HERMES and COMPASS, is shown in Fig. 17. The data available cover the interval between $0.004 < x < 0.3$ and the task of

the future JLab12 will be to map precisely the full valence region, where effects are large and supposed to drop quite fast.

The high luminosity of JLab should also help to better constrain the transverse momentum dependence of the Sivers function. At large hadron transverse momentum, *i.e.* $P_{hT} \gg \Lambda_{\text{QCD}}$, the transverse-momentum dependence of the various factors in the factorisation formula [20] may be calculated from perturbative QCD. Following Ji-Qiu-Vogelsang-Yuan [144], the $\sin(\phi - \phi_S)$ azimuthal modulation of Sivers should behave as:

$$\langle \sin(\phi - \phi_S) \rangle|_{P_{hT} \gg \Lambda_{\text{QCD}}} \propto \frac{1}{P_{hT}}. \quad (10)$$

in the region $\Lambda_{\text{QCD}} \ll P_{hT} \ll Q$. The above result holds also when the transverse momentum is compatible with the large-scale Q . Measurement of the P_{hT} dependence of the Sivers asymmetry will, thus, allow to check the predictions of a unified description of SSA [20,144,145] and will study the transition from a non-perturbative to a perturbative description. Measurement of the P_{hT} -dependence of the Sivers asymmetry with much higher precision that

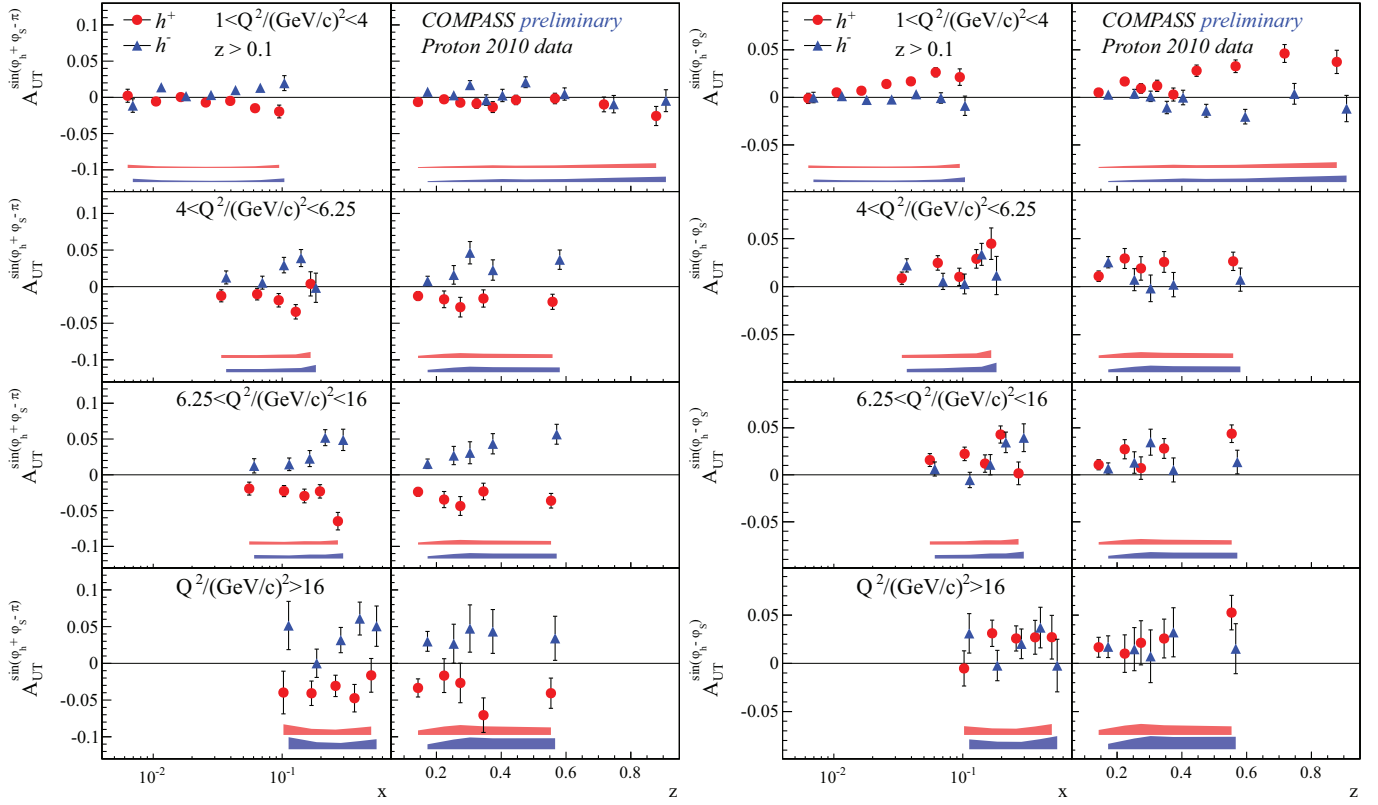


Fig. 16. Collins (left) and Sivers (right) asymmetries for 4 Q^2 bins as a function of x and z .

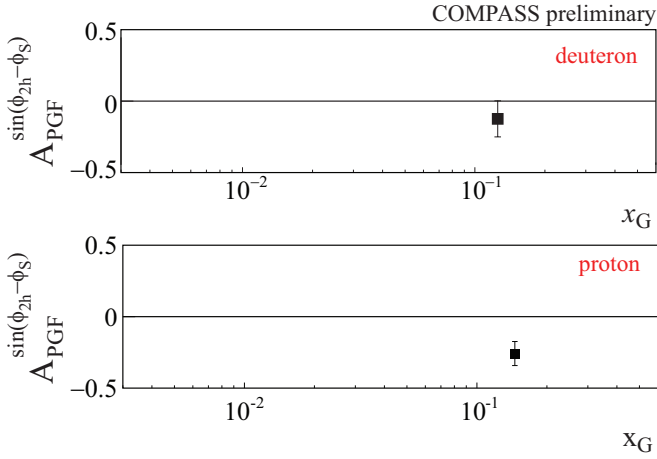


Fig. 15. COMPASS Sivers asymmetry for gluons on deuterons (top) and on protons (bottom). While the deuteron result is negative but still compatible with zero, a clear negative signal is visible for the protons.

the existing one would also allow one to determine the first moment of the Sivers function, which also has a direct connection to so-called soft gluon pole matrix elements [13, 146, 147] :

$$f_{1T}^{\perp(1)}(x) = \int d^2 k_{\perp} \frac{k_{\perp}^2}{2M^2} f_{1T}^{\perp(1)}(x, k_{\perp}^2) . \quad (11)$$

Making such a cross check is crucial to understand the various transverse single-spin phenomena in semi-inclusive reactions by means of perturbative QCD. The P_{hT} -dependence will thus provide access to the k_{\perp} -dependence of the Sivers function, which may be relevant to resolve the so-called “sign mismatch”, or the observed mismatch between the signs of the moment of the Sivers function extracted from SIDIS data and twist-3 calculations [148].

At Jefferson Lab there are several closely-related proposals approved to measure spin and azimuthal asymmetries in all three Halls, providing complementary studies of different aspects of the complex structure of the nucleon in terms of flavour, momentum and spin. Hall-A has an extensive SIDIS program to access TMDs with polarised targets.

Two proposals have been approved to study SSAs with SoLID detector using transversely [149] and longitudinally [150] polarised ^3He targets. Another Hall-A proposal has been approved [151] to measure SSAs on a transversely polarised ^3He target, using the Super-Bigbite spectrometer with kaon identification using a RICH detector.

A proposal using the SoLID detector and transversely polarised NH_3 target [152], with similar goals and kinematic coverage has been also approved by JLab PAC. SoLID proposal offers higher statistics in the intermediate P_{hT} and Q^2 range, while CLAS12 proposal will access higher P_{hT} and Q^2 with negligible nuclear background, allowing to probe the same physics with completely different systematics. The future data from Hall-A experi-

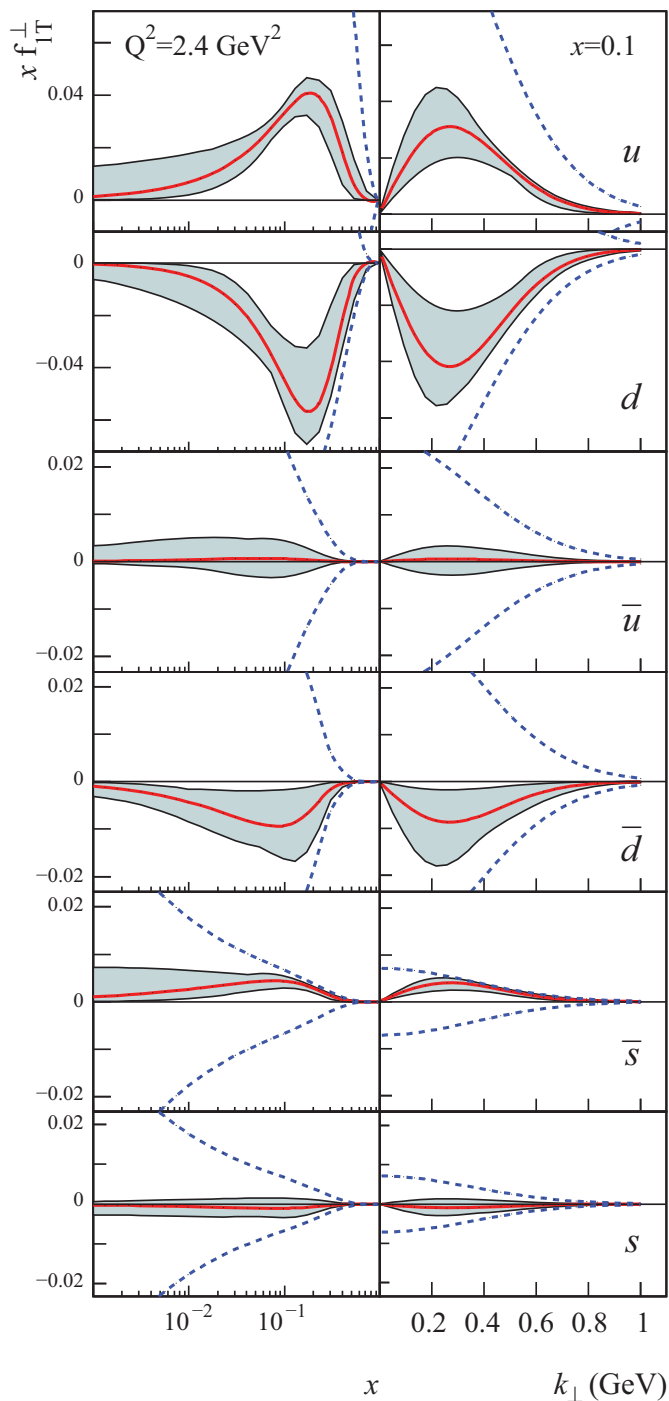


Fig. 17. Sivers function for quark/antiquark flavours as extracted in [128].

ments will be complementary to those from the proposed CLAS12 measurement with transversely polarised hydrogen target.

The large acceptance of CLAS12 will allow measurements of SIDIS pions over a wide range in x, Q^2 and hadron transverse momenta, where the spin-orbit correlations and corresponding SSAs are expected to be significant. The crucial advantages of the proposed configura-

tion using HD-Ice target is the large acceptance (no strong holding field is required) and the negligible nuclear background, in particular for large P_{hT} . Worth noticing that the HD-Ice dilution factor, which is a crucial element for precision studies of transverse momentum dependence of TMDs, is a factor of 2 better of the nuclear targets (NH_3, ND_3) at small P_{hT} of hadrons, and goes up to a factor of 6 at $P_{hT} > 0.8$ GeV [78], due to increasing fraction of pions coming from nuclear target at large P_{hT} . The projected CLAS12 statistical precision on the Sivers A_{UT} SSA for pions and charged kaons on a proton target, corresponding to 100 days of data-taking with the HD-Ice target, are shown in Fig. 18.

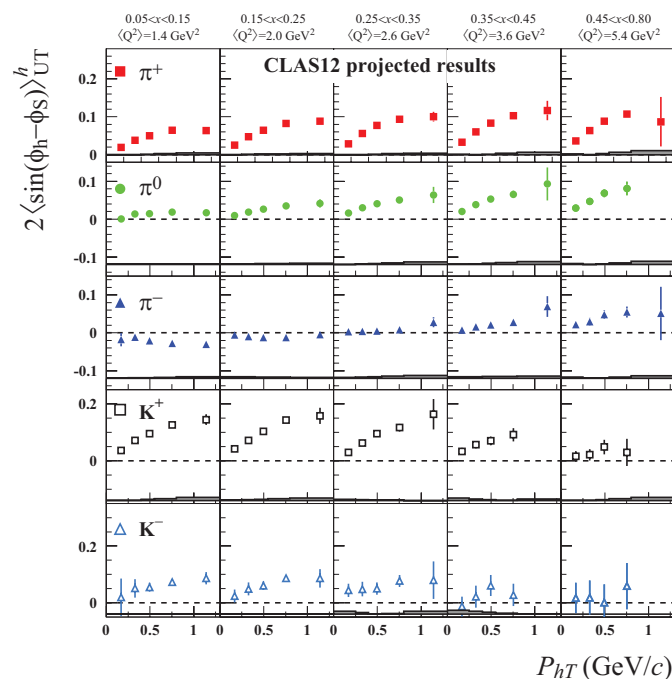


Fig. 18. Expected 2-dimensional projections for the Sivers amplitudes for some typical bins from CLAS12 (based on the use of a phenomenological model for the Sivers function [128]). Bins in x as a function of P_{hT} . Estimates of the expected systematic uncertainties (global acceptance and detector smearing effects) are also shown.

Thanks to the high statistics achievable in 100 days of measurements, a 4-dimensional analysis of the extracted azimuthal moments can be performed. This allows the disentanglement of all the specific kinematic dependences and a deeper inspection of the mechanisms generating the asymmetries. In the proposed data-taking time, a precise mapping of a large portion of the phase-space is achievable for pions, extending into the high- Q^2 high- P_{hT} region of interest. In particular a precision of few percents can be obtained at large Q^2 for values of P_{hT} up to 1 GeV/c. The x and Q^2 variables are typically correlated by the detector acceptance. Noteworthy, the statistics of the proposed experiment allows to subdivide each x -bin in several Q^2 -bins thus disentangling the two kinematic dependences.

An extended mapping is possible also in the kaon sector, although with a precision limited by the smaller yields.

A wide range in Q^2 provided by the CLAS12 detector at JLab would also allow studies of Q^2 -evolution. The projected Q^2 -dependence of the Sivers function as measured by the CLAS12 data is shown in Fig. 19. Studies of the Q^2 dependence will be required also to constrain the higher-twist contributions. Measuring the Q^2 -dependence of the Sivers function is one of the main goals of the upgraded CLAS12 experiment using a transversely polarised HD target [153].

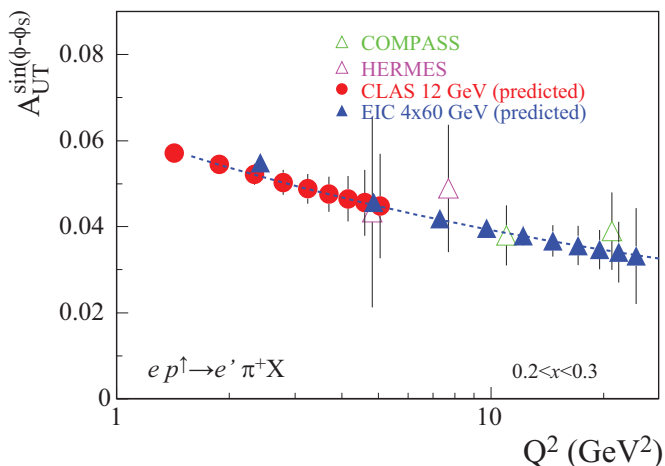


Fig. 19. Projections for the Sivers amplitudes as a function of Q^2 in the valence region for CLAS12 and EIC, compared to existing measurements at HERMES and COMPASS.

3.5 Measuring TMDs: the Boer Mulders distribution

Already in the early days of the parton model it was realized that the inclusion of quark intrinsic transverse momentum leads to modifications of the cross sections in lepton-nucleon deep-inelastic scattering. Cosine modulations in the azimuthal dependencies of the distribution of the produced hadrons about the direction of the virtual photon can be non-vanishing due to simple kinematic effects (Cahn effect) [154,155]. It was also later realized that the interplay between the parton transverse momentum and spin (Boer-Mulders effect [8]) can generate a leading-twist (unsuppressed in $1/Q$) contribution to the $\cos 2\phi$ modulations:

$$F_{UU}^{\cos 2\phi} = C \left[-\frac{2(\hat{\mathbf{h}} \cdot \mathbf{k}_\perp)(\hat{\mathbf{h}} \cdot \mathbf{k}_\perp) - \mathbf{k}_\perp \cdot \mathbf{p}_\perp}{MM_h} h_1^\perp H_1^\perp \right] \quad (12)$$

Perturbative-QCD effects, like gluon radiation, can also lead to azimuthal dependencies in the semi-inclusive DIS cross section. However, they contribute mainly at large values of P_{hT} , and are next-to-leading order in the strong coupling constant.

Among the various contributions suppressed as $1/Q$, several involve either a distribution or fragmentation function that relates to quark-gluon-quark correlations, and hence is interaction dependent and has no probabilistic interpretation. In the Wandzura-Wilczek approximation [156] all these terms are neglected, and only two contributions are considered:

$$F_{UU}^{\cos \phi} \simeq -\frac{2M}{Q} C \left[\frac{\hat{\mathbf{h}} \cdot \mathbf{p}_\perp}{M} f_1 D_1 + \frac{\hat{\mathbf{h}} \cdot \mathbf{k}_\perp}{M_h} h_1^\perp H_1^\perp \right] \quad (13)$$

where the first (second) term is related to the Chan (Boer-Mulders) effect. There are no contributions to $F_{UU}^{\cos 2\phi}$ at a suppression $1/Q$. Not all contributions beyond a suppression of $1/Q$ have been calculated, however a contribution suppressed as $1/Q^2$ is expected from the Cahn effect to $F_{UU}^{\cos 2\phi}$.

In Drell-Yan experiments, non-zero azimuthal modulations have been measured [157–162] that violate the Lam-Tung relation [163]. Such a violation can be ascribed to the Boer-Mulders distribution function [164]. Sizable modulations have been extracted in pion-induced Drell-Yan reactions, where a valence quark and a valence antiquark annihilate. At a variance, when a sea parton is involved as in proton-induced Drell-Yan processes, the measured modulations become smaller. This behaviour can be explained by a small Boer-Mulders function for the sea partons.

Only a few measurements of cosine modulations in semi-inclusive DIS experiments have been published in the past [165–168]. Most measurements averaged over any possible flavour dependence as they refer to hadrons without type nor charge distinction, and only to hydrogen target or hydrogen and deuterium targets combined together.

Several precise SIDIS measurements have become available. The CLAS collaboration measured non-zero cosine modulations for positive pions produced by 6 GeV/c electrons scattering off the proton [169]. The HERMES experiment have measured cosine modulations of hadrons produced in the scattering of 27.5 GeV/c electrons and positrons off pure hydrogen and deuterium targets, where the lepton beam scatters directly off neutrons and protons (with only negligible nuclear effects in case of deuterium) [170]. For the first time these modulations were determined in a four-dimensional kinematic space for positively and negatively charged pions and kaons separately, as well as for unidentified hadrons. At COMPASS, positive and negative hadrons produced by the 160 GeV/c muon beam scattering off a ${}^6\text{LiD}$ target have been measured in a three-dimensional grid of the relevant kinematic variables x , z and P_{hT} [35].

In all the experiments, the new data confirm the existence of a sizeable $\cos \phi$ and a not-zero $\cos 2\phi$ modulations. However, the results published by different experiment appear not fully consistent. For example, positive $\cos 2\phi$ amplitudes for both positively and negatively charged hadrons were measured at COMPASS. At HERMES, positive $\cos 2\phi$ amplitudes are extracted for negatively charged pions, while for positively charged pions the

moments are compatible with zero, but tend to be negative in some kinematic regions. In all the cases, the amplitudes of the cosine modulations show strong kinematic dependencies. Comparisons between COMPASS and HERMES $\cos\phi$ and $\cos 2\phi$ modulations for hadrons in the almost overlapping kinematic region ($0.02 < x < 0.13$, $\langle Q^2 \rangle \simeq 4$ $(\text{GeV}/c)^2$ of COMPASS and $0.023 < x < 0.145$, $\langle Q^2 \rangle \simeq 2$ $(\text{GeV}/c)^2$ of HERMES) are shown in Figs. 20 and 21, for P_{hT} ranges below 0.5 (GeV) , and above 0.5 (GeV) , respectively. The multidimensional results of the two experiments are corrected point-to-point for the ratio of the longitudinal to transverse virtual photon flux before making the weighting average with the statistical error only in x and P_{hT} . At low- P_{hT} there is an overall agreement in the z -dependence between the two experiments, with the exception of the $\cos 2\phi$ modulation of positive hadrons (that show the same behaviour but have an off-set of about 0.05). The same is true also for $P_{hT} > 0.5$ GeV/c , even if some point-to-point disagreement is visible for positive hadrons (we have to keep in mind that systematic errors are not shown). Given the difficulties of these measurement, one has to keep in mind that, in order to perform a more complete and fair comparison between results and between results and theoretical models, a full differential analysis, using the complete multi-dimensional information provided by the experiments in public databases, is mandatory.

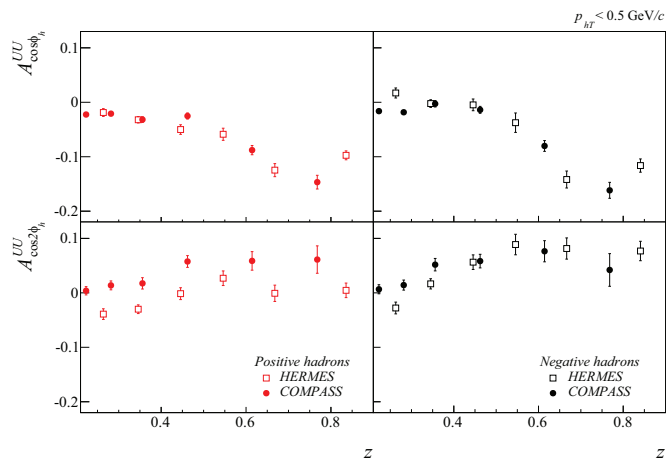


Fig. 20. $\cos\phi$ (upper row) and $\cos 2\phi$ (lower row) positive (left) and negative (right) hadron modulation averaged for $P_{hT} < 0.5$ GeV/c and in the region of $0.02 < x < 0.13$, $\langle Q^2 \rangle \simeq 4$ $(\text{GeV}/c)^2$ (for COMPASS [35]) and $0.023 < x < 0.145$, $\langle Q^2 \rangle \simeq 2$ $(\text{GeV}/c)^2$ (for HERMES [170]). Only statistical errors are shown.

The large $\cos\phi$ amplitude implies that the contribution suppressed with powers of $1/Q$, as the ones discussed in Eq. 13, are not negligible. This largely complicates the interpretation as there could be several additional contributions at sub-leading order which are not calculable [171]. Nevertheless some attempts have been made to explain the main features of the resulting modulations, i.e. the sizeable changes with hadron type and charge. The similarity

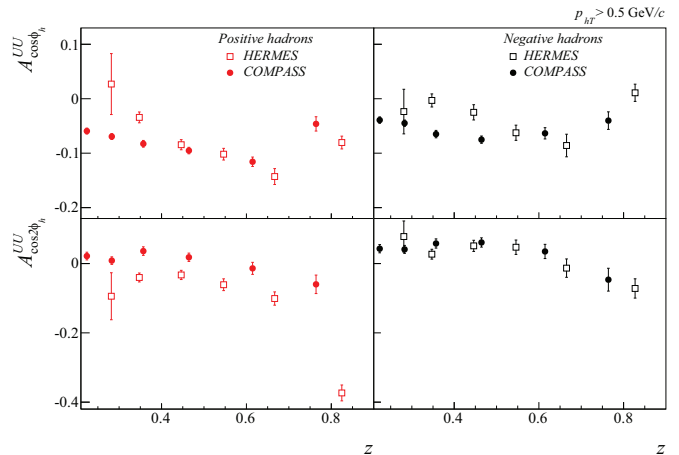


Fig. 21. $\cos\phi$ (upper row) and $\cos 2\phi$ (lower row) positive (left) and negative (right) hadron modulation averaged for $P_{hT} > 0.5$ GeV/c and in the region of $0.02 < x < 0.13$, $\langle Q^2 \rangle \simeq 4$ $(\text{GeV}/c)^2$ (for COMPASS [35]) and $0.023 < x < 0.145$, $\langle Q^2 \rangle \simeq 2$ $(\text{GeV}/c)^2$ (for HERMES [170]). Only statistical errors are shown.

between hydrogen and deuterium results seems to indicate that the Boer-Mulders distribution function has the same sign for up and down quarks, in agreement with expectations from theoretical considerations [172,173]. The difference between charged pion results may be ascribed to the Boer-Mulders term, due to the dominating contribution of the up quark in SIDIS reactions and the opposite sign of Collins fragmentation of up quark into positively and negatively charged pions. The striking difference between kaon and pion $\cos 2\phi$ modulations measured at HERMES does not find an explanation on the peculiar Collins fragmentation as the B-factories find similar asymmetries between the two meson types [118,174].

A step forward will be possible by new complementary measurements. New Drell-Yan experiments offer the opportunity to study azimuthal modulations and the Lam-Tung relation with unprecedented precision [175,176]. At JLab, several experiments are planned to study in detail the unpolarised SIDIS azimuthal modulations for different hadron types in a broad kinematic range [60,109].

3.6 Measuring TMDs: pretzelocity

Studies of the shape of the proton indicate [177,178] that for transversely polarised quarks in a transversely polarised nucleon, the shape of the nucleon is reminiscent of a pretzel. The distribution of transversely polarised quarks in a transversely polarised nucleon is described by the TMD $h_{1T}^\perp(x, k_\perp^2)$ and its magnitude will thus be related to the “pretzelocity” of the proton [177]. Recently it has been suggested, based on some quark models, that the pretzelocity TMD may also be related to the quark orbital angular momentum (OAM) [37,179–181]

$$\mathcal{L}_z^q = - \int dx d^2k_\perp \frac{k_\perp^2}{2M^2} h_{1T}^{\perp q}(x, k_\perp^2). \quad (14)$$

The TMD h_{1T}^\perp corresponds to the amplitude where the nucleon and active quark longitudinal polarisations flip in opposite directions, involving therefore a change by two units of OAM between the initial and final nucleon states; it gives therefore an indication about the ‘sphericity’ of the nucleon. This asymmetry is expected to be suppressed by a scaling factor of P_{hT}^2 with respect to the Sivers and Collins asymmetries in the region of small hadron transverse momenta of $P_{hT} < 1$ GeV/c. It was shown (see *e.g.* [182]) that in a gauge theory, in general, \mathcal{L}_z^q may not be related to the total quark contribution to the nucleon spin from a combination of GPDs from Ji’s sum-rule [183].

Preliminary COMPASS [184,185] and HERMES [186] measurements of this asymmetry are compatible with a null result within the statistical accuracy both on deuteron and proton targets. Projections for approved JLab12 measurements for transverse target asymmetries [152, 153], sensitive to pretzelocity distribution $h_{1T}^\perp(x, k_\perp^2)$ are shown in Fig. 22.

3.7 Measuring TMDs: worm-gear or Kotzinian-Mulders distributions

Spin-orbit correlations are accessible in SIDIS with longitudinally polarised target in measurements of double and single-spin asymmetries. For a longitudinally polarised target the only azimuthal asymmetry arising in leading order is the $\sin 2\phi$ moment,

$$F_{UL}^{\sin 2\phi} = C \left[-\frac{2(\hat{\mathbf{h}} \cdot \mathbf{k}_\perp)(\hat{\mathbf{h}} \cdot \mathbf{k}_\perp) - \mathbf{k}_\perp \cdot \mathbf{p}_\perp}{MM_h} h_{1L}^\perp H_1^\perp \right] \quad (15)$$

The distribution function giving rise to SSA, h_{1L}^\perp , is related to the real part of the interference of wave functions for different orbital momentum states, and describes transversely polarised quarks in the longitudinally polarised nucleon. The physics of $F_{UL}^{\sin 2\phi}$, which involves the Collins fragmentation function H_1^\perp and the distribution function h_{1L}^\perp , was first discussed by Kotzinian and Mulders in 1996 [6, 7, 188]. The same distribution function is accessible in double polarised Drell-Yan, where it gives rise to the $\cos 2\phi$ azimuthal moment in the cross section [189]. The behaviour of the Kotzinian-Mulders distribution function has been studied both in large- x [190] and large N_c [191] limits of QCD. It involves helicity flip of the quarks but is diagonal in the nucleon helicity. One of the characteristic features of h_{1L}^\perp is that it has no analogues in the spin densities related to the GPDs in the impact parameter space [192, 193]. The results in the light-cone quark model [40] for the densities with transversely polarised quarks in a longitudinally polarised proton shown in Fig. 23 are in good agreement with recent lattice calculation [41, 42]. For the density related to h_{1L}^\perp , they predict shifts of similar magnitude of $\langle \mathbf{k}_x^u \rangle = -60(5)$ MeV, and $\langle \mathbf{k}_x^d \rangle = 15(5)$ MeV.

Measurements of the $\sin 2\phi$ SSA [188], allows the study of the Collins effect with no contamination from other

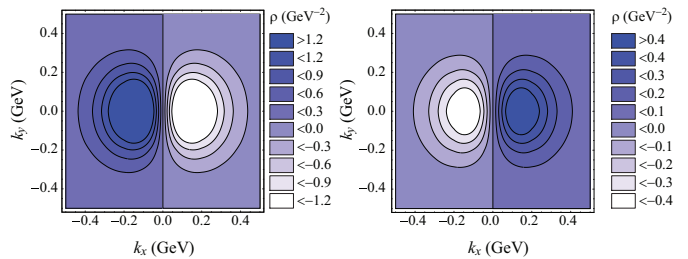


Fig. 23. Quark densities in the \mathbf{k}_T plane for transversely polarised quarks in a longitudinally polarised proton for up (left panel) and down (right panel) quark [40].

mechanisms. During the last few years, first results on longitudinal target SSAs have become available from HERMES, COMPASS and CLAS [27, 34, 104, 194, 195]. Measurement of the $\sin 2\phi$ moment in the relatively low x -range by HERMES [194] and COMPASS [104] are small and consistent with zero (Fig. 24).

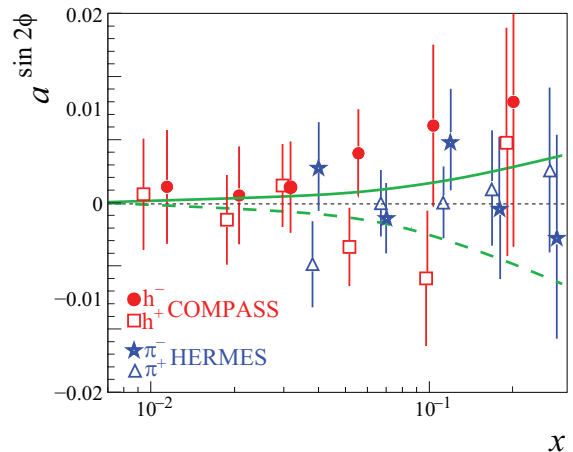


Fig. 24. Dependence of the modulation amplitude $a^{\sin 2\phi}$ on x from COMPASS [104] for charged hadrons and HERMES [105] for charged pions; also shown are the calculations of Ref. [196].

A measurably large asymmetry has been predicted only at large x ($x > 0.2$), a region well-covered by JLab [38, 196–200]. The data from CLAS at 6 GeV indicate large azimuthal moments both for $\sin \phi$ and $\sin 2\phi$ [27]. The phenomenological studies of the $\sin 2\phi_h$ asymmetry in the longitudinally polarised SIDIS process [27, 105, 194] have been performed in [38, 196, 201, 202] and recently in [203], showing that the asymmetry may be around several per cent.

An approved CLAS12 experiment [106] will simultaneously collect data on $\mathbf{p}, \mathbf{d}(e, e'\pi^{+,0,-})$. The predictions have been obtained with a full simulation of the hadronisation process [204] and the acceptance of CLAS12 for all particles (Fig.25). Calculations were done using h_{1L}^\perp from the chiral quark soliton model evolved to $Q^2=1.5$ GeV² [197], f_1 from GRV95 [205], and D_1 from Kretzer, Leader, and Christova [206]. The curves correspond to dominance of the favoured fragmentation $H_1^{\perp u \rightarrow \pi^+}$. An important ingre-

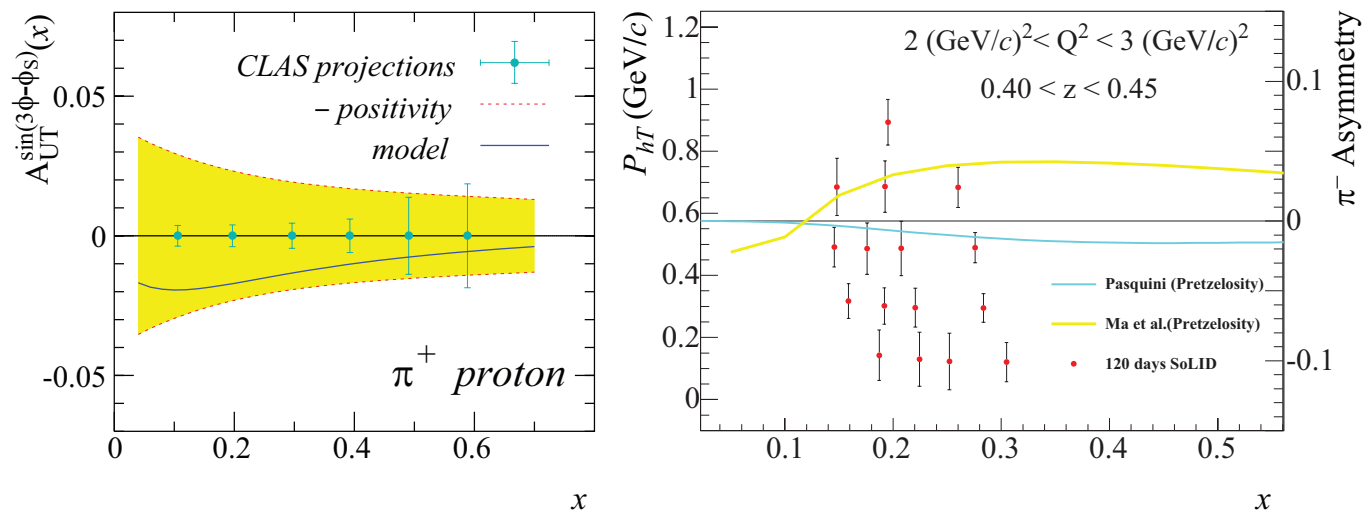


Fig. 22. The $A_{UT}^{\sin(3\phi-\phi_s)}$ asymmetry in π^+ electro-production from proton target in the kinematics of CLAS12 as function of x [180] for a bin in P_{hT} ($0.45 < P_{hT} < 0.6$). Solid curve presents the prediction of relativistic covariant model [187]. The shaded area is the region allowed by positivity. Left panel shows projections for SOLID for some typical bins for π^+ and π^- .

dent for the estimates are so-called ‘‘Lorentz-invariance relations’’ that connect h_{1L}^\perp with h_1 [7]. Meanwhile these relations are known not to be valid exactly [12, 207]. It is of importance to find out experimentally to which extent such relations can provide useful approximations, or whether they are badly violated.

junction with the spin-independent fragmentation function D_1 , in double-spin asymmetries with a longitudinally polarised beam and a transversely polarised nucleon. The joint use of a transversely polarised target and a longitudinally polarised beam will also allow for measurements of the double-spin asymmetry, A_{LT} , in the same kinematic region:

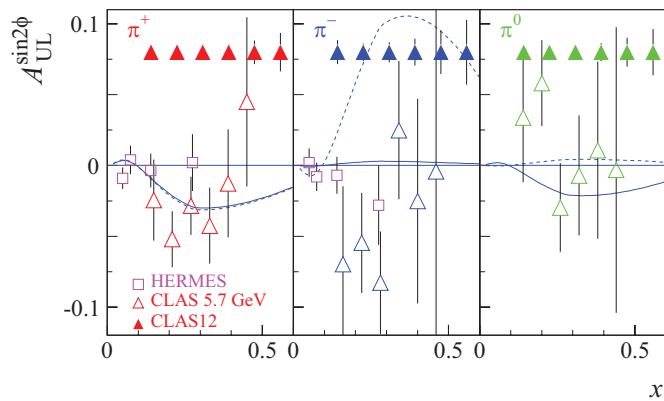


Fig. 25. The projected x -dependence of the target SSA at 11 GeV. The triangles illustrate the expected statistical accuracy. The open squares and triangles show the existing measurement of the Kotzinian-Mulders asymmetries from HERMES and the preliminary results from CLAS 5.7 GeV CLAS data sets [27], respectively. The curves are calculated using Ref. [208].

Another interesting TMD distribution function accessible in studies with transversely polarised nucleons is the *worm-gear* $g_{1T}^\perp(x, k_\perp^2)$. It describes the probability to find longitudinally polarised quarks in a transversely polarised nucleon. Noteworthy, it is the only TMD function not affected by initial- or final-state interactions as it is neither chiral-odd nor T-odd. It can be accessed, in con-

$$A_{LT} = \frac{1}{f P_B P_t} \frac{(N^{+\uparrow} + N^{-\downarrow}) - (N^{+\downarrow} + N^{-\uparrow})}{(N^{+\uparrow} + N^{-\downarrow}) + (N^{+\downarrow} + N^{-\uparrow})} \quad (16)$$

where P_B is the electron beam polarisation, and $N^{\pm\uparrow\downarrow}$ is the extracted number of ehX events for positive (+) or negative (−) helicities of the beam electrons and transverse (\uparrow, \downarrow) target polarisations. Recent measurements of the double-spin asymmetry A_{LT} for charged pion electro-production in SIDIS on a transversely polarised ^3He target, performed at Hall-A of JLab indicate a positive azimuthal asymmetry for π^- production on ^3He and the neutron, while the π^+ asymmetries were found to be consistent with zero [29].

Preliminary COMPASS measurement [185] of $A_{LT}^{\cos(\phi-\phi_s)}$ for protons is shown in Fig. 26. The statistical uncertainties of all LT-asymmetries are larger than the other SSAs due to the smaller $D(y)$ factors and the lepton beam polarisation of $\simeq 80\%$. Nevertheless a non-zero trend at relatively large x -region is visible.

SIDIS measurements at JLab with a joint use of a transversely polarised target and a longitudinally polarised beam provide access to the leading-twist TMD $g_{1T}^q(x)$. Significant A_{LT} double-spin asymmetries were predicted for the CLAS12 kinematics (see Fig. 27).

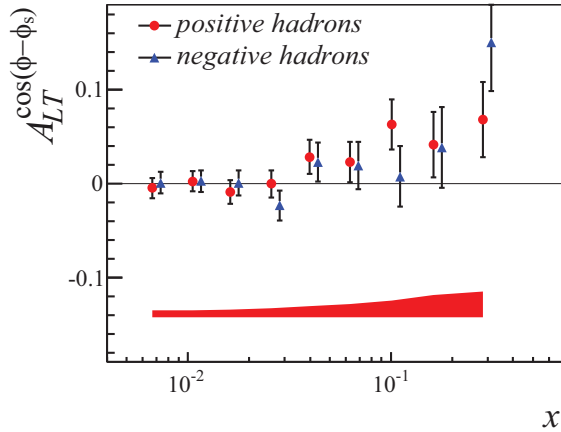


Fig. 26. Preliminary COMPASS [185] $A_{LT}^{\cos(\phi_h - \phi_s)}$ asymmetry vs. x . Systematic uncertainties are shown by the coloured band.

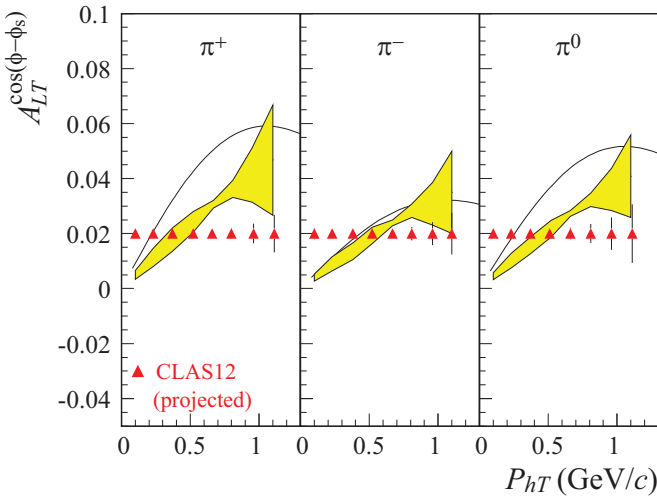


Fig. 27. Expected statistical uncertainties for the $A_{LT}^{\cos(\phi - \phi_s)}$ amplitudes sensitive to the g_{1T}^{\perp} TMD as a function of x . Overlaid are also a band from calculations [209] of g_{1T}^{\perp} based on two transverse-momentum Gaussian widths ($\langle k_{\perp}^2 \rangle = 0.15$ and 0.25 GeV^2). The curve is from light-cone constituent quark model [38].

4 Towards extraction of TMDs from multi-dimensional SIDIS data

Measurements of amplitudes for identified pions and kaons provide and will provide precious information not only on the contribution to the distribution functions involved from the various quark flavours (e.g., it would allow for constraints on the contribution from the strange sea quarks), but also on the ratio of favoured to unfavoured polarised fragmentation functions, complementary to e^+e^- data.

The width of the k_{\perp} distribution for different partonic distributions can be different. Values for different T-even TMDs, have been computed [38] in the constituent quark model [40], indicating differences in widths of quark distributions between 10-30% [40].

A common assumption is the Gaussian ansatz for the transverse momentum dependence of distribution and frag-

mentation functions with the average $\langle P_{hT} \rangle$ of hadrons produced in SIDIS given by Eq.7. In the approximation of flavour and x or z -independent widths, a satisfactory description of HERMES deuteron data on average P_{hT} [105] was obtained [210] with

$$\langle k_{\perp}^2 \rangle = 0.33 \text{ GeV}^2, \quad \langle p_{\perp}^2 \rangle = 0.16 \text{ GeV}^2. \quad (17)$$

Very similar results were obtained in Ref. [125] from a study of EMC data [166] on the Cahn effect. Although the ansatz seems to describe satisfactorily the present available data sets [36], it has to be considered as an approximation.

A comprehensive study of the nucleon structure should consider the role of the quark flavour. The use of different targets in conjunction with the detection of various hadrons in the final state provide access to statistical information about the flavour of the struck quark. In particular, kaons provide enhanced sensitivity on strangeness in the matter (partonic sea of the nucleon) and in the vacuum (through fragmentation). Kaon detection is generally challenged by the about one order of magnitude larger flux of pions. Thus very little is known about the spin-orbit correlations related to the strange quark. Only recently dedicated measurements have become available and, despite the limited statistical accuracy, in most of the cases they show surprising results. This is an indication of a non trivial role of the sea quarks in the nucleon, or of a peculiar behaviour of the fragmentation mechanism in the presence of strange quark. Moreover a hint exists that kaons provide enhanced sensitivity on higher-twist effects [23]. Only the ability to explore the relevant kinematic dependence of experiments coping high-luminosity with large-acceptance and particle identification will allow to shed light on the interpretation. Precision measurement of the Q -dependence of the asymmetries, in particular, will allow to isolate higher-twist effects, while measuring the P_{hT} -dependence over a large range will allow to map the transition between perturbative and non-perturbative regime.

Single-spin asymmetries were also investigated in inclusive electro-production of charged pions and kaons from transversely polarised protons at the HERMES experiment and JLab [211,212]. The data sample are dominated by the kinematic regime $Q^2 \sim 0$ GeV^2 of quasi-real photo-production, where P_{hT} is the only hard scale. The origin of the observed asymmetries can, therefore, most likely be explained by higher-twist contributions. These type of measurements may provide a test of TMD factorisation in processes with single large scale (P_{hT}) and provide additional information for a consistent understanding of the large SSAs measured in the single inclusive production of large P_{hT} hadrons in proton-proton collisions [213]. Very significant higher-twist azimuthal modulations have been observed by all lepton production experiments. In addition to the $F_{UU}^{\cos\phi}$ [35] and $F_{LU}^{\sin\phi}$ (Fig.6), discussed above, significant non zero contributions have been observed for $F_{UL}^{\sin\phi}$ [194,195] and $F_{UT}^{\sin\phi_S}$ structure functions [24,214]. Higher-twists are indispensable part of SIDIS analysis (see Eq 1) and their understanding is crucial for interpretation of SIDIS leading-twist observables.

Very little is known about polarisation dependent fragmentation functions (i.e. Collins), but an effort is being pursued to extract them from the large sample of data collected at B-factories [118, 119]. Very precise information on the fragmentation process is anticipated in the next future thanks to the approval of Super B-factories. The detailed study can be completed only by SIDIS measurements, which constrain the fragmentation functions at much lower centre-of-mass energy with specific flavour sensitivity (not accessible in e^+e^- reactions). The detailed knowledge of the fragmentation process would reflect on the precise determination of parton distributions only at experiments with enough statistical precision and flavour sensitivity (like CLAS12) and even in this case, only if TMD evolution will be known at the same level of precision.

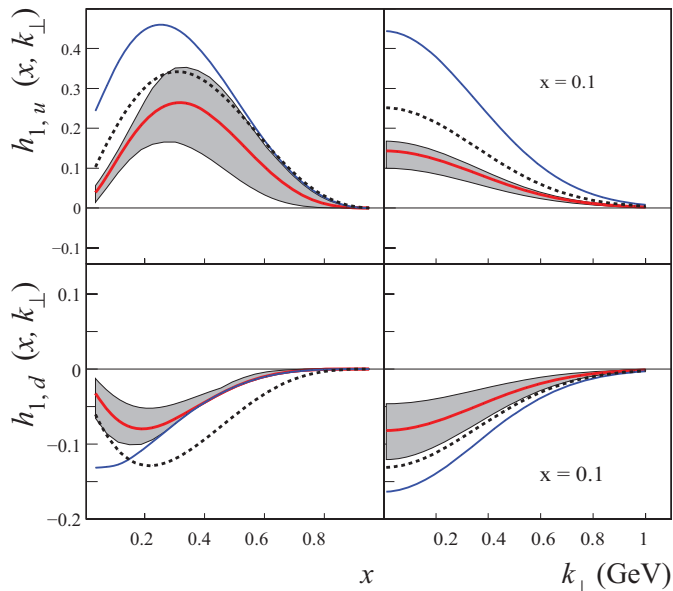


Fig. 28. Transversity distribution functions for u and d flavours as extracted in [122].

The extraction of the transversity from $A_{UT}^{\sin(\phi+\phi_S)}$ requires parametrisation for the unpolarised distribution and fragmentation functions along with approximations for the essentially unknown polarised T-odd chiral-odd Collins fragmentation function H_1^\perp . The first extraction of the transversity distribution, together with the Collins fragmentation function, has been carried out recently [121, 122] through a global fit of the BELLE data from e^+e^- annihilation and the HERMES [22] and COMPASS [25, 101, 184] data on semi-inclusive DIS, see Figs. 28-29. Transversity distributions for u and d quarks and Collins fragmentation functions from current experimental data have been extracted recently, applying the TMD evolution in the Collins-Soper-Sterman formalism, in a global analysis of the Collins asymmetries in back-to-back di-hadron productions in e^+e^- annihilation measured by BELLE and

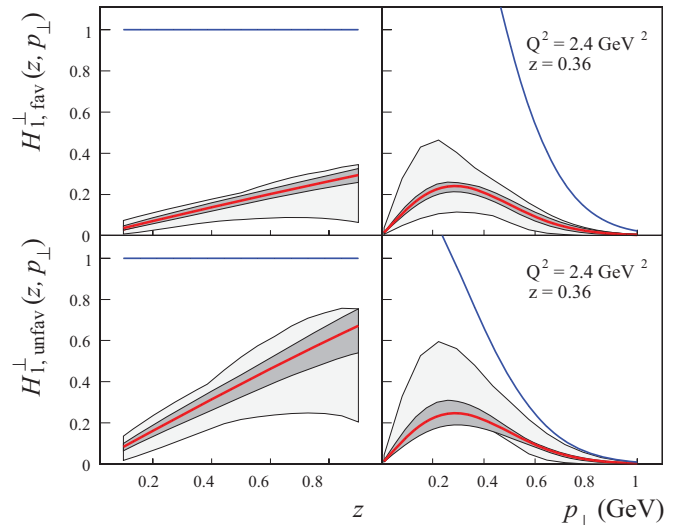


Fig. 29. Favoured and unfavoured Collins fragmentation functions as extracted in [122].

BABAR Collaborations and SIDIS data from HERMES, COMPASS, and JLab HALL A experiments.

The Collins SSA for positive kaons is similar to that of positive pions in sign and magnitude, a result compatible with the dominance of the u -flavour in lepto-scattering over a proton target. However, at HERMES the signal for π^- and K^- are found to follow a different behaviour, the former being large and negative, the latter being basically compatible with zero with a hint to be positive [24]. The result would be interesting since the K^- has no valence quarks in common with the target proton and sea quark transversity is expected to be small, thus K^- brings specific sensitivity on rank-2 Collins function. Note that the knowledge of the Collins function has an impact on the extraction of all the chirally-odd TMD parton distributions. The results for K^- are still controversial, since COMPASS data [215] can not prove or disprove it, although seem to not support the HERMES hint. The issue can be solved only by increasing the statistical accuracy.

Although spin asymmetries are typically not too sensitive to acceptance and radiative corrections, in the case of the transverse SSA where a large number of contributions appear as different azimuthal moments in the cross section, the acceptance and radiative corrections are more important. The analysis of the transverse target data requires fits in the 2-dimensional space of the relevant azimuthal angles ϕ and ϕ_S . COMPASS was designed from the beginning to have a full 2π azimuthal acceptance and a very large acceptance on the polar angle (from within the beam up to 200 mrad) to fully cover the current fragmentation region. On the other side, a detailed procedure on the accounting for acceptance corrections in the separation of the different azimuthal moments was developed by the HERMES collaboration [24]. According to this method, a fully-differential (thus virtually free from acceptance effects) parametrisation of the asymmetries is extracted from the data itself with a fully-unbinned max-

imum likelihood fit. The parametrisation is then used in input to an originally unpolarised Monte Carlo simulation which accounts for a complete model of the instrumental effects (acceptance, smearing, inefficiencies...) to generate a pseudo-data sample. The systematic effects are evaluated as the difference of the asymmetries extracted from the pseudo-data sample and the parametrisation in input to the Monte Carlo. Accounting for all the relevant azimuthal moments in the MC generator, it will be crucial also to properly handle the radiative effects.

4.1 Systematic Errors

The systematic uncertainties can be divided into two categories: those that scale with the measured asymmetry and those that are independent of the measured results. In the first category, the dominant uncertainty is expected to be that from the target polarisation and the dilution from the target material other than polarised hydrogen or deuterium.

One of the main contributions to the estimated relative uncertainties comes from the procedure used to separate the azimuthal moments of interest from other, potentially non-zero, azimuthal asymmetries (for example a twist-3 $\sin(\phi_S)$ moment or radiative effects). Another large contribution is from possible contamination of the SIDIS pion event sample by pions from decays of diffractive vector mesons, mainly ρ^0 (the contamination for kaons is expected to be much smaller). Large acceptance detectors (like COMPASS and CLAS12) measure simultaneously the asymmetries from background processes, such as ρ^0 production, and use that info for corrections, as the size of the contamination can be measured as well. With high luminosity also the SIDIS vector meson asymmetries can be studied with precision, and are the matter of the di-hadron proposals (discussed in a separate contribution).

The real photon emission from the lepton and hadron legs as well as by additional virtual particle contributions is changing the SIDIS kinematics. Since most of the outgoing particles in SIDIS remain undetected, events with the real photon emission can not be removed experimentally. The contribution of events with an additional exchange of virtual particles cannot be removed at all. As a result the measured SIDIS cross section includes not only the lowest order contribution but also the higher order effects whose contribution has to be accounted in the data analysis. The corresponding radiative corrections (RC) have to be calculated theoretically. The primary step in the solution of the task on RC calculation in the lepton nucleon scattering assumes the calculation of the part of the total lowest order QED correction that includes real photon emission from lepton leg as well as the additional virtual photon between the initial and final leptons and the correction due to virtual photon self-energy. Other types of RC, such as box-type contribution or real photon emission from hadrons, are less important, as these corrections do not contain the leading order contribution which is proportional to the logarithm of the lepton mass, and therefore,

their contribution is much smaller comparing to RC from lepton part.

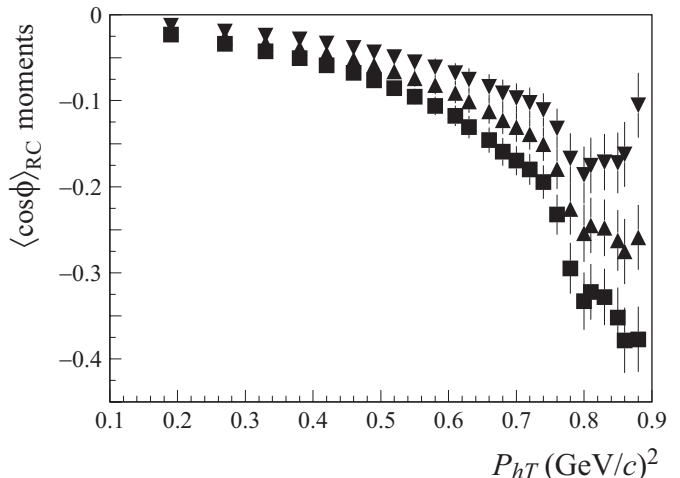


Fig. 30. The pion transverse momentum dependence of the $\cos \phi$ -moment in JLab12 kinematics at $x = 0.3$ and $z = 0.3$, generated by radiation of additional photon calculated from haprad2.0 [216] for three different structure functions with $\cos \phi$ input amplitudes equal to -5% (squares), -10% (triangles up), and -15% (triangles down).

As a matter of fact, the radiative effects in SIDIS also generate azimuthal moments which may couple with the moments in the Born cross section and produce more complex azimuthal structure in the observed cross section [216, 217]. Azimuthal moment generated by radiative effects, and their sensitivity to different input ϕ -dependent structure functions are shown on Fig.30.

For COMPASS the errors on the target polarisation and dilution are estimated to be about 5%, while the point-to-point systematic effects have an upper limit ranging between 50 to 70% of the statistical accuracy. The average total relative systematic error on the proton SSAs has been estimated for CLAS12 measurements to be of order 7%, mostly dominated by errors on the target polarisation, nuclear background and acceptance corrections (4% each). That should be sufficiently small for a very significant measurement.

4.2 Fourier Transformed Cross Sections

TMDs and transverse momentum-dependent fragmentation functions enter the SIDIS cross section in a convolution with respect to transverse momentum. In order to extract TMDs, it is therefore advantageous to project the differential cross section onto Fourier modes [218]. The result is a product of TMDs and fragmentation functions in Fourier space. Choosing different values of the parameter b_T , the Fourier transform of the transverse momentum k_{\perp} , would allow to scan the transverse momentum dependence of the distributions in Fourier space [219, 220].

The b_T -dependent distributions are also the objects that appears in the evolution equations that describe the scale dependence beyond tree level, see, e.g., Ref. [221]. Lattice calculations of TMDs are performed in b -space rather than momentum space as well [41, 43]. This suggests that it is the b_T -dependent quantities that are most suitable for a model independent analysis and comparison with lattice data.

This new extraction framework has a very different systematic, and can be used to check the standard procedures for TMD extraction, in particular extraction of k_\perp -dependence of TMDs. The main questions to address when applying this procedure to SIDIS data (in particular CLAS12 data) are the limited range in hadron transverse momenta and the low Q^2 , as Fourier-transformed quantities receive (through the Fourier integral) contributions from the entire range of P_{hT} , while the whole factorisation formalism requires $P_{hT} \ll Q$. Due to contributions to the cross section at high $|P_{hT}|$ that are not accounted for in the TMD factorised framework, further studies are needed as to whether and in what range of b_T we can extract TMDs in Fourier space at JLab kinematics with moderate theoretical uncertainties. Precision measurements at large b_T may require precision measurements at P_{hT} in the range of 1.2-1.5 GeV, limiting the minimum Q^2 to at least 2 GeV².

A reanalysis of the data using using Fourier transformed cross sections is also planned in COMPASS. This experiment is also working on P_{hT} -weighted asymmetries; building single spin asymmetries by weighting the cross section with P_{hT} dependent weights results in a direct connection of the amplitude of the azimuthal modulation to a product of moments of PDFs and FFs [8, 222] instead of a convolution over the intrinsic transverse momenta. The differences with respect to standard TMD extractions will again allow to check systematic effects in different procedures.

5 Summary

We have partially reviewed many results and progresses in the field of transverse momentum dependent distribution and fragmentation functions.

At least two striking effects have been demonstrated in the last years, i.e.: there is a non zero correlation between the spin of transversely polarised quarks and the P_{hT} of the hadrons created in the hadronisation process, with evidences coming both from SIDIS processes on transversely polarised nucleons and high energy e^+e^- annihilation into hadrons. This correlation has allowed the extractions of trasversity. There is a non-zero correlation between the spin of a transversely polarised nucleon and the intrinsic transverse momentum of the quarks, giving rise to the Sivers asymmetry. This has been the starting point to draw increasing attention to TMDs.

The measurements of single-spin asymmetries in lepto-production of hadrons performed by HERMES and COMPASS collaborations, and JLab experiments have shown

that spin-orbit and quark-gluon correlations are very significant in kinematic regions where the valence quark contributions are significant. Analysis of measured single-spin asymmetries provided first glimpse of transverse momentum distributions of quarks in polarised and unpolarised nucleons. First extraction of TMDs from HERMES and COMPASS data revealed once again the complexity of the strong dynamics inside the nucleon and therefore importance of a common TMD extraction framework. To progress further we need multi-dimensional results that are starting to come from COMPASS and HERMES and will come with high precision from JLab12, combining experiments with unpolarised [59, 60, 109], longitudinally polarised [106, 107] and transversely polarised [150, 153, 223]. One of the main focuses of the proposed measurement will be the transverse momentum dependence of the underlying TMDs, and in particular of the Sivers function. The analysis of these data sets will require understanding of evolution properties of TMDs and large k_\perp corrections, control of various subleading $1/Q^2$ corrections, radiative corrections and knowledge of involved transverse momentum dependent fragmentation functions.

The measurements of single and double spin asymmetries for pions and kaons in a large range of kinematic variables combined with measurements with unpolarised targets, will provide detailed information on the flavour and polarisation dependence of the transverse momentum distributions of quarks in the valence region and, in particular, on the x and k_\perp dependence of the leading TMD parton distribution functions of u and d quarks. Such measurements allow for detailed tests of QCD dynamics in the valence region, complementing the information obtained from inclusive DIS. They also serve as novel tools for exploring nuclear structure in terms of the quark and gluon degrees of freedom.

Together with the multi-dimensional results from HERMES and COMPASS, COMPASS phase-II and the proposed experiments at upgraded JLab will provide statistically significant measurements of the kinematic dependences of single and double spin azimuthal asymmetries in pion and kaon lepto-production in SIDIS. The large acceptance of the detectors permits a simultaneous scan of various variables (x , z , P_{hT} and Q^2), crucial for studies of transverse momentum dependence of TMDs. Combination of measurements in a large Q^2 range would allow studies of evolution effects and control possible higher-twist contributions in the measurements of TMD observables in general, and of the Sivers asymmetry in particular.

Analysis of already existing electro-production data from HERMES, COMPASS and JLab with unpolarised and polarised targets has shown that the proposed measurements are feasible. Combined analysis of all three data sets will constrain different TMDs and relations between them, providing important input to global analysis of PDFs and will provide a substantial contribution to a full tomography of the nucleon.

One of the most striking predictions of the theory, is the sign change of Sivers and Boer-Mulders TMDs in SIDIS and Drell-Yan reactions, which can be used for test-

ing the QCD TMD factorization and the TMD approach itself. The experimental proof that the present LO approach to TMD is correct is presently missing and we are eagerly waiting for results of the running (like COMPASS) or planned polarised Drell-Yan experiments.

References

1. I. Garzia and F. Giordano, *This EPJ* (2015).
2. U.D. E.C Aschenauer and F. Murgia, *This EPJ* (2015).
3. M. Diehl, *This EPJ* (2015).
4. J.P. Ralston and D.E. Soper, *Nucl. Phys. B*152 (1979) 109.
5. D.W. Sivers, *Phys. Rev. D*41 (1990) 83.
6. A. Kotzinian, *Nucl. Phys. B*441 (1995) 234, [hep-ph/9412283](#).
7. P.J. Mulders and R.D. Tangerman, *Nucl. Phys. B*461 (1996) 197, [hep-ph/9510301](#).
8. D. Boer and P.J. Mulders, *Phys. Rev. D*57 (1998) 5780, [arXiv:hep-ph/9711485](#).
9. P.J. Mulders and J. Rodrigues, *Phys. Rev. D*63 (2001) 094021, [hep-ph/0009343](#).
10. A.V. Belitsky, X.d. Ji and F. Yuan, *Phys. Rev. D*69 (2004) 074014, [hep-ph/0307383](#).
11. A. Bacchetta et al., *JHEP* 02 (2007) 093, [hep-ph/0611265](#).
12. K. Goeke, A. Metz and M. Schlegel, *Phys. Lett. B*618 (2005) 90, [hep-ph/0504130](#).
13. S. Meissner, A. Metz and K. Goeke, *Phys. Rev. D*76 (2007) 034002, [hep-ph/0703176](#).
14. C. Lorce and B. Pasquini, *Phys.Rev. D*84 (2011) 034039, [arXiv:1104.5651](#).
15. V. Barone, A. Drago and P.G. Ratcliffe, *Phys. Rept.* 359 (2002) 1, [hep-ph/0104283](#).
16. V. Barone, F. Bradamante and A. Martin, *Prog.Part.Nucl.Phys.* 65 (2010) 267, [arXiv:1011.0909](#).
17. J.C. Collins, *Nucl. Phys. B*396 (1993) 161, [hep-ph/9208213](#).
18. S.M. Aybat and T.C. Rogers, *Phys.Rev. D*83 (2011) 114042, [arXiv:1101.5057](#).
19. P. Sun and F. Yuan, *Phys.Rev. D*88 (2013) 034016, [arXiv:1304.5037](#).
20. X. Ji, J. Ma and F. Yuan, *Phys. Rev. D*71 (2005) 034005, [hep-ph/0404183](#).
21. J.C. Collins and D.E. Soper, *Nucl. Phys. B*193 (1981) 381.
22. HERMES Collaboration, A. Airapetian et al., *Phys. Rev. Lett.* 94 (2005) 012002, [hep-ex/0408013](#).
23. HERMES Collaboration, A. Airapetian et al., *Phys. Rev. Lett.* 103 (2009) 152002, [arXiv:0906.3918](#).
24. HERMES Collaboration, A. Airapetian et al., *Phys. Lett. B*693 (2010) 11, [arXiv:1006.4221](#).
25. COMPASS Collaboration, V.Y. Alexakhin et al., *Phys. Rev. Lett.* 94 (2005) 202002, [hep-ex/0503002](#).
26. COMPASS Collaboration, M.G. Alekseev et al., *Phys. Lett. B*692 (2010) 240, [arXiv:1005.5609](#).
27. CLAS Collaboration, H. Avakian et al., *Phys. Rev. Lett.* 105 (2010) 262002, [arXiv:1003.4549](#).
28. Hall A Collaboration, X. Qian et al., *Phys. Rev. Lett.* 107 (2011) 072003, [arXiv:1106.0363](#).
29. Hall A Collaboration, J. Huang et al., *Phys. Rev. Lett.* 108 (2012) 052001, [arXiv:1108.0489](#).
30. Hall A Collaboration, Y.X. Zhao et al., *Phys. Rev. C*90 (2014) 055201, [arXiv:1404.7204](#).
31. Hall A Collaboration, Y. Zhang et al., *Phys. Rev. C*90 (2014) 055209, [arXiv:1312.3047](#).
32. CLAS Collaboration, H. Avakian et al., *Phys. Rev. D*69 (2004) 112004, [hep-ex/0301005](#).
33. Hall A Collaboration, Y.X. Zhao et al., (2015), [arXiv:1502.01394](#).
34. HERMES Collaboration, A. Airapetian et al., *Phys. Lett. B*622 (2005) 14, [hep-ex/0505042](#).
35. COMPASS Collaboration, C. Adolph et al., *Nucl. Phys. B*886 (2014) 1046, [arXiv:1401.6284](#).
36. P. Schweitzer, T. Teckentrup and A. Metz, *Phys. Rev. D*81 (2010) 094019, [arXiv:1003.2190](#).
37. H. Avakian et al., *Phys. Rev. D*81 (2010) 074035, [arXiv:hep-ph/1001.5467](#).
38. S. Boffi et al., *Phys. Rev. D*79 (2009) 094012, [arXiv:hep-ph/0903.1271](#).
39. B. Pasquini and F. Yuan, *Phys. Rev. D*81 (2010) 114013, [arXiv:1001.5398](#).
40. B. Pasquini, S. Cazzaniga and S. Boffi, *Phys. Rev. D*78 (2008) 034025, [arXiv:hep-ph/0806.2298](#).
41. P. Hagler et al., *Europhys. Lett.* 88 (2009) 61001, [arXiv:hep-lat/0908.1283](#).
42. B.U. Musch, (2009), [arXiv:0907.2381](#).
43. B.U. Musch et al., *Phys. Rev. D*83 (2011) 094507, [arXiv:1011.1213](#).
44. Z. Lu and B.Q. Ma, *Nucl. Phys. A*741 (2004) 200, [hep-ph/0406171](#).
45. M. Anselmino et al., *Phys. Rev. D*74 (2006) 074015, [hep-ph/0608048](#).
46. C. Bourrely, F. Buccella and J. Soffer, *Phys.Rev. D*83 (2011) 074008, [arXiv:1008.5322](#).
47. M. Wakamatsu, *Phys. Rev. D*79 (2009) 094028, [arXiv:0903.1886](#).
48. P. Schweitzer, M. Strikman and C. Weiss, *JHEP* 1301 (2013) 163, [arXiv:1210.1267](#).
49. H. Mkrtchyan et al., *Phys. Lett. B*665 (2008) 20, [arXiv:hep-ph/0709.3020](#).
50. HERMES Collaboration, A. Airapetian et al., *Phys.Rev. D*87 (2013) 074029, [arXiv:1212.5407](#).
51. COMPASS Collaboration, C. Adolph et al., *Eur.Phys.J. C*73 (2013) 2531, [arXiv:1305.7317](#).
52. M. Anselmino et al., *JHEP* 1404 (2014) 005, [arXiv:1312.6261](#).
53. A. Signori et al., *JHEP* 1311 (2013) 194, [arXiv:1309.3507](#).
54. H.H. Matevosyan et al., *Phys.Rev. D*85 (2012) 014021, [arXiv:1111.1740](#).
55. Belle Collaboration, M. Leitgab et al., *Phys. Rev. Lett.* 111 (2013) 062002, [arXiv:1301.6183](#).
56. BaBar Collaboration, J.P. Lees et al., *Phys. Rev. D*88 (2013) 032011, [arXiv:1306.2895](#).
57. N. Makke, (2014), [arXiv:1411.4244](#).
58. COMPASS Collaboration, F. Gautheron et al., (2010), COMPASS-II Proposal.
59. R. Ent, P. Bosted and H. Mkrtchyan, *JLab Experiment E12-09-017* (2009).
60. H. Avakian et al., *JLab Experiment E12-09-008* (2009).
61. R. Ent et al., *JLab Experiment E12-06-104* (2006).
62. J. Collins, *Foundations of perturbative QCD* (Cambridge University Press, 2011).

63. M.G. Echevarria et al., *Eur.Phys.J. C* 73 (2013) 2636, [arXiv:1208.1281](#).
64. S.M. Aybat, A. Prokudin and T.C. Rogers, *Phys.Rev.Lett.* 108 (2012) 242003, [arXiv:1112.4423](#).
65. A. Schafer and J. Zhou, *Phys. Rev. D* 88 (2013) 074012, [arXiv:1305.5042](#).
66. Z.t. Liang, X.N. Wang and J. Zhou, *Phys. Rev. D* 77 (2008) 125010, [arXiv:hep-ph/0801.0434](#).
67. S. Kretzer, *Phys. Rev. D* 62 (2000) 054001, [arXiv:hep-ph/0003177](#).
68. M. Hirai et al., *Phys.Rev. D* 75 (2007) 094009, [arXiv:hep-ph/0702250](#).
69. D. de Florian, R. Sassot and M. Stratmann, *Phys.Rev. D* 75 (2007) 114010, [arXiv:hep-ph/0703242](#).
70. HERMES Collaboration, A. Airapetian et al., *Nucl.Phys. B* 780 (2007) 1, [arXiv:0704.3270](#).
71. HERMES Collaboration, A. Airapetian et al., *Eur.Phys.J. A* 47 (2011) 113, [arXiv:1107.3496](#).
72. N.B. Chang, W.T. Deng and X.N. Wang, *Phys.Rev. C* 89 (2014) 034911, [arXiv:1401.5109](#).
73. JET Collaboration, K.M. Burke et al., *Phys. Rev. C* 90 (2014) 014909, [arXiv:1312.5003](#).
74. PHENIX Collaboration, A. Adare et al., *Phys. Rev. Lett.* 101 (2008) 232301, [arXiv:0801.4020](#).
75. PHENIX Collaboration, A. Adare et al., *Phys. Rev. C* 87 (2013) 034911, [arXiv:1208.2254](#).
76. ALICE Collaboration, B. Abelev et al., *Phys. Lett. B* 720 (2013) 52, [arXiv:1208.2711](#).
77. CMS Collaboration, S. Chatrchyan et al., *Eur. Phys. J. C* 72 (2012) 1945, [arXiv:1202.2554](#).
78. W.K. Brooks and H. Hakobyan, *Nucl. Phys. A* 830 (2009) 361c, [arXiv:0907.4606](#).
79. HERMES Collaboration, A. Airapetian et al., *Phys.Lett. B* 684 (2010) 114, [arXiv:0906.2478](#).
80. J.H. Gao, Z.t. Liang and X.N. Wang, *Phys. Rev. C* 81 (2010) 065211, [arXiv:1001.3146](#).
81. Y.k. Song, Z.t. Liang and X.N. Wang, (2014), [arXiv:1402.3042](#).
82. A. Accardi et al., JLab LoI LOI12-14-004 (2014).
83. W. Brooks et al., JLab Experiment E12-14-001 (2014).
84. I.I. Balitsky and L.N. Lipatov, *Sov. J. Nucl. Phys.* 28 (1978) 822, [*Yad. Fiz.* 28,1597(1978)].
85. S. Catani, M. Ciafaloni and F. Hautmann, *Phys. Lett. B* 307 (1993) 147.
86. H1 and ZEUS Collaboration, F. Aaron et al., *JHEP* 1001 (2010) 109, [arXiv:0911.0884](#).
87. ZEUS, H1, H. Abramowicz et al., *Eur. Phys. J. C* 73 (2013) 2311, [arXiv:1211.1182](#).
88. F. Hautmann and H. Jung, *Nucl. Phys. B* 883 (2014) 1, [arXiv:1312.7875](#).
89. S. Dooling, F. Hautmann and H. Jung, *Phys. Lett. B* 736 (2014) 293, [arXiv:1406.2994](#).
90. ATLAS Collaboration, G. Aad et al., *Phys. Rev. D* 85 (2012) 092002, [arXiv:1201.1276](#).
91. CMS Collaboration, V. Khachatryan et al., *Phys. Lett. B* 741 (2015) 12, [arXiv:1406.7533](#).
92. I.I. Balitsky et al., *Phys. Rev. Lett.* 77 (1996) 3078, [hep-ph/9605439](#).
93. R. Ent, *This EPJ* (2015).
94. Spin Muon, B. Adeva et al., *Phys. Lett. B* 420 (1998) 180, [hep-ex/9711008](#).
95. E142 Collaboration, P.L. Anthony et al., *Phys. Rev. Lett.* 71 (1993) 959.
96. E143 Collaboration, K. Abe et al., *Phys. Rev. D* 58 (1998) 112003, [hep-ph/9802357](#).
97. HERMES Collaboration, A. Airapetian et al., *Phys. Rev. D* 71 (2005) 012003, [hep-ex/0407032](#).
98. CLAS Collaboration, R. Fatemi et al., *Phys. Rev. Lett.* 91 (2003) 222002, [nucl-ex/0306019](#).
99. Hall A Collaboration, X. Zheng et al., *Phys. Rev. C* 70 (2004) 065207, [nucl-ex/0405006](#).
100. CLAS, Y. Prok et al., *Phys. Rev. C* 90 (2014) 025212, [arXiv:1404.6231](#).
101. COMPASS Collaboration, E.S. Ageev et al., *Nucl. Phys. B* 765 (2007) 31, [hep-ex/0610068](#).
102. COMPASS Collaboration, M.G. Alekseev et al., *Phys. Lett. B* 690 (2010) 466, [arXiv:1001.4654](#).
103. COMPASS Collaboration, C. Adolph et al., (2015), [arXiv:1503.08935](#).
104. M.G. Alekseev et al., *Eur. Phys. J. C* 70 (2010) 39, [arXiv:1007.1562](#).
105. HERMES Collaboration, A. Airapetian et al., *Phys. Lett. B* 562 (2003) 182, [hep-ex/0212039](#).
106. H. Avakian et al., JLab Experiment E12-07-107 (2007).
107. H. Avakian et al., JLab Experiment E12-09-009 (2009).
108. D. Boer et al., (2011), [arXiv:1108.1713](#).
109. H. Avakian et al., JLab Experiment E12-06-112 (2006).
110. J. Zhou, F. Yuan and Z.T. Liang, *Phys. Rev. D* 81 (2010) 054008, [arXiv:hep-ph/0909.2238](#).
111. A. Accardi et al., (2012), [arXiv:1212.1701](#).
112. HERMES Collaboration, A. Airapetian et al., *Phys. Lett. B* 648 (2007) 164, [hep-ex/0612059](#).
113. R.L. Jaffe and X.D. Ji, *Nucl. Phys. B* 375 (1992) 527.
114. E. Leader, A.V. Sidorov and D.B. Stamenov, *Phys. Lett. B* 462 (1999) 189, [hep-ph/9905512](#).
115. H.C. Kim, M.V. Polyakov and K. Goeke, *Phys. Lett. B* 387 (1996) 577, [hep-ph/9604442](#).
116. Belle Collaboration, K. Abe et al., *Phys. Rev. Lett.* 96 (2006) 232002, [hep-ex/0507063](#).
117. Belle Collaboration, A. Ogawa et al., *AIP Conf. Proc.* 915 (2007) 575.
118. Belle Collaboration, R. Seidl et al., *Phys. Rev. D* 78 (2008) 032011, [arXiv:0805.2975](#).
119. I. Garzia et al., *Nuovo Cimento* 33C (2010) 269.
120. BaBar Collaboration, I. Garzia, *Nuovo Cim.* C036 (2013) 181.
121. M. Anselmino et al., *Phys.Rev. D* 75 (2007) 054032, [arXiv:hep-ph/0701006](#).
122. M. Anselmino et al., *Nucl. Phys. Proc. Suppl.* 191 (2009) 98, [arXiv:0812.4366](#).
123. B. Andersson et al., *Phys. Rept.* 97 (1983) 31.
124. X. Artru, (2010), [arXiv:1001.1061](#).
125. M. Anselmino et al., *Phys. Rev. D* 71 (2005) 074006, [hep-ph/0501196](#).
126. J.C. Collins et al., *Phys. Rev. D* 73 (2006) 094023, [hep-ph/0511272](#).
127. W. Vogelsang and F. Yuan, *Phys. Rev. D* 72 (2005) 054028, [hep-ph/0507266](#).
128. M. Anselmino et al., *Eur.Phys.J. A* 39 (2009) 89, [arXiv:0805.2677](#).
129. COMPASS Collaboration, C. Adolph et al., *Phys.Lett. B* 717 (2012) 383, [arXiv:1205.5122](#).
130. COMPASS Collaboration, M. Alekseev et al., *Phys. Lett. B* 673 (2009) 127, [arXiv:0802.2160](#).
131. COMPASS Collaboration, C. Adolph et al., *Phys. Lett. B* 744 (2015) 250, [arXiv:1408.4405](#).

132. M. Anselmino, M. Boglione and S. Melis, Phys.Rev. D86 (2012) 014028, [arXiv:1204.1239](#).
133. M.G. Echevarria et al., Phys.Rev. D89 (2014) 074013, [arXiv:1401.5078](#).
134. S.M. Aybat et al., Phys.Rev. D85 (2012) 034043, [arXiv:1110.6428](#).
135. COMPASS Collaboration, A. Szabelski, EPJ Web Conf. 85 (2015) 02006.
136. COMPASS Collaboration, C. Adolph et al., Phys. Rev. D87 (2013) 052018, [arXiv:1211.6849](#).
137. COMPASS Collaboration, C. Adolph et al., Phys. Lett. B718 (2013) 922, [arXiv:1202.4064](#).
138. S.J. Brodsky and S. Gardner, Phys. Lett. B643 (2006) 22, [arXiv:hep-ph/0608219](#).
139. M. Anselmino et al., Phys.Rev. D74 (2006) 094011, [arXiv:hep-ph/0608211](#).
140. Fermilab E906/SeaQuest, P. Reimer et al., (2001), Fermilab Proposal 906, Unpublished.
141. E906/SeaQuest, P. Reimer et al., (2006), Experiment update to Fermilab PAC.
142. L. Blandt et al., (2011).
143. D. Boer, (2011), [arXiv:1105.2543](#).
144. X. Ji et al., Phys. Rev. D73 (2006) 094017, [hep-ph/0604023](#).
145. J. Collins and T. Rogers, Phys. Rev. D91 (2015) 074020, [arXiv:1412.3820](#).
146. J.w. Qiu and G.F. Sterman, Phys. Rev. Lett. 67 (1991) 2264.
147. D. Boer, P.J. Mulders and F. Pijlman, Nucl. Phys. B667 (2003) 201, [hep-ph/0303034](#).
148. Z.B. Kang et al., Phys. Rev. D83 (2011) 094001, [arXiv:1103.1591](#).
149. H. Hao, Q. X. and P. J.-C., JLab Experiment E12-11-007 (2008).
150. J.P. Chen et al., JLab Experiment E12-11-007 (2008).
151. G. Cates et al., JLab Experiment E12-11-007 (2008).
152. X. Li et al., JLab Experiment E12-11-108 (2011).
153. H. Avakian et al., JLab Experiment C12-11-111 (2011).
154. R.N. Cahn, Phys. Lett. B78 (1978) 269.
155. R.N. Cahn, Phys. Rev. D40 (1989) 3107.
156. S. Wandzura and F. Wilczek, Phys. Lett. B72 (1977) 195.
157. NA10, S. Falciano et al., Z. Phys. C31 (1986) 513.
158. NA10 Collaboration, M. Guanziroli et al., Z. Phys. C37 (1988) 545.
159. J.S. Conway et al., Phys. Rev. D39 (1989) 92.
160. J.G. Heinrich et al., Phys. Rev. D44 (1991) 1909.
161. NuSea Collaboration, L.Y. Zhu et al., Phys. Rev. Lett. 99 (2007) 082301, [arXiv:hep-ex/0609005](#).
162. NuSea Collaboration, L.Y. Zhu et al., Phys. Rev. Lett. 102 (2009) 182001, [arXiv:0811.4589](#).
163. C.S. Lam and W.K. Tung, Phys. Rev. D21 (1980) 2712.
164. D. Boer and P.J. Mulders, Nucl. Phys. B569 (2000) 505, [arXiv:hep-ph/9906223](#).
165. European Muon, J.J. Aubert et al., Phys. Lett. B130 (1983) 118.
166. European Muon, M. Arneodo et al., Z. Phys. C34 (1987) 277.
167. E665, M.R. Adams et al., Phys. Rev. D48 (1993) 5057.
168. ZEUS, J. Breitweg et al., Phys. Lett. B481 (2000) 199, [hep-ex/0003017](#).
169. CLAS Collaboration, M. Osipenko et al., Phys. Rev. D80 (2009) 032004, [arXiv:hep-ex/0809.1153](#).
170. HERMES Collaboration, A. Airapetian et al., Phys.Rev. D87 (2013) 012010, [arXiv:1204.4161](#).
171. V. Barone, S. Melis and A. Prokudin, Phys. Rev. D81 (2010) 114026, [arXiv:0912.5194](#).
172. M. Burkardt, Phys. Rev. D72 (2005) 094020, [hep-ph/0505189](#).
173. M. Burkardt and B. Hannafious, Phys. Lett. B658 (2008) 130, [arXiv:0705.1573](#).
174. BaBar Collaboration, J.P. Lees et al., Phys. Rev. D90 (2014) 052003, [arXiv:1309.5278](#).
175. Fermilab E906/SeaQuest Collaboration, W. Lorenzon, Nuovo Cim. C035N2 (Lorenzon:2012zz 2012) 231.
176. COMPASS Collaboration, M. Quaresma, EPJ Web Conf. 73 (2014) 02010.
177. G.A. Miller, Phys. Rev. C76 (2007) 065209, [arXiv:nucl-th/0708.2297](#).
178. M. Burkardt, hep-ph 0709.2966 (2007), [arXiv:hep-ph/0709.2966](#).
179. J. She, J. Zhu and B.Q. Ma, Phys. Rev. D79 (2009) 054008, [arXiv:0902.3718](#).
180. H. Avakian et al., Phys.Rev. D78 (2008) 114024, [arXiv:0805.3355](#).
181. H. Avakian et al., Mod. Phys. Lett. A24 (2009) 2995, [arXiv:0910.3181](#).
182. M. Burkardt and H. BC, Phys. Rev. D79 (2009) 071501, [arXiv:0812.1605](#).
183. X.D. Ji, Phys. Rev. Lett. 78 (1997) 610, [hep-ph/9603249](#).
184. COMPASS, B. Parsamyan, Eur. Phys. J. ST 162 (2008) 89, [arXiv:0709.3440](#).
185. B. Parsamyan, PoS DIS2013 (2013) 231, [arXiv:1307.0183](#).
186. HERMES, G. Schnell, PoS DIS2010 (2010) 247.
187. A. Efremov et al., AIP Conf.Proc. 1149 (2009) 547, [arXiv:0812.3246](#).
188. A.M. Kotzinian and P.J. Mulders, Phys. Rev. D54 (1996) 1229, [hep-ph/9511420](#).
189. R.D. Tangerman and P.J. Mulders, Phys. Rev. D51 (1995) 3357, [hep-ph/9403227](#).
190. S.J. Brodsky and F. Yuan, Phys. Rev. D74 (2006) 094018, [hep-ph/0610236](#).
191. P.V. Pobylitsa, hep-ph/0301236 (2003), [arXiv:hep-ph/0301236](#).
192. M. Diehl and P. Hagler, Eur. Phys. J. C44 (2005) 87, [hep-ph/0504175](#).
193. B. Pasquini and S. Boffi, Phys. Lett. B653 (2007) 23, [arXiv:0705.4345](#).
194. HERMES Collaboration, A. Airapetian et al., Phys. Rev. Lett. 84 (2000) 4047, [hep-ex/9910062](#).
195. HERMES Collaboration, A. Airapetian et al., Phys. Rev. D64 (2001) 097101, [hep-ex/0104005](#).
196. H. Avakian et al., Phys. Rev. D77 (2008) 014023, [arXiv:hep-ph/0709.3253](#).
197. A.V. Efremov, K. Goeke and P. Schweitzer, Phys. Rev. D67 (2003) 114014, [hep-ph/0208124](#).
198. L.P. Gamberg, G.R. Goldstein and M. Schlegel, Phys. Rev. D77 (2008) 094016, [arXiv:hep-ph/0708.0324](#).
199. A.V. Efremov et al., Phys. Rev. D80 (2009) 014021, [arXiv:hep-ph/0903.3490](#).
200. J. Zhu and B.Q. Ma, (2011), [arXiv:1104.5545](#).
201. B.Q. Ma, I. Schmidt and J.J. Yang, Phys. Rev. D63 (2001) 037501, [hep-ph/0009297](#).
202. B.Q. Ma, I. Schmidt and J.J. Yang, Phys. Rev. D65 (2002) 034010, [hep-ph/0110324](#).

203. J. Zhu and B.Q. Ma, Phys. Lett. B696 (2011) 246, [arXiv:1104.4564](#).
204. L. Mankiewicz, A. Schafer and M. Veltri, Comput. Phys. Commun. 71 (1992) 305.
205. M. Gluck et al., Phys. Rev. D53 (1996) 4775, [hep-ph/9508347](#).
206. S. Kretzer, E. Leader and E. Christova, Eur. Phys. J. C22 (2001) 269, [hep-ph/0108055](#).
207. K. Goeke et al., Phys. Lett. B567 (2003) 27, [hep-ph/0302028](#).
208. A.V. Efremov, K. Goeke and P. Schweitzer, Czech. J. Phys. 55 (2005) A189, [hep-ph/0412420](#).
209. A. Kotzinian, B. Parsamyan and A. Prokudin, Phys. Rev. D73 (2006) 114017, [hep-ph/0603194](#).
210. J.C. Collins et al., Phys. Rev. D73 (2006) 014021, [hep-ph/0509076](#).
211. HERMES Collaboration, A. Airapetian et al., Phys. Lett. B728 (2014) 183, [arXiv:1310.5070](#).
212. Hall A Collaboration, K. Allada et al., Phys. Rev. C89 (2014) 042201, [arXiv:1311.1866](#).
213. M. Anselmino et al., Phys. Rev. D81 (2010) 034007, [arXiv:0911.1744](#).
214. HERMES Collaboration, A. Airapetian et al., Phys.Lett. B682 (2010) 345, [arXiv:0907.2596](#).
215. COMPASS Collaboration, C. Schill et al., (2011), [arXiv:DIS 2011 Conference](#).
216. I. Akushevich, A. Ilyichev and M. Osipenko, Phys.Lett. B672 (2009) 35, [arXiv:0711.4789](#).
217. I. Akushevich, N. Shumeiko and A. Soroko, Eur. Phys. J. C10 (1999) 681, [hep-ph/9903325](#).
218. D. Boer et al., JHEP 1110 (2011) 021, [arXiv:1107.5294](#).
219. D. Boer et al., (2011), [in preparation](#).
220. M. Aghasyan et al., (2014), [arXiv:1409.0487](#).
221. A. Idilbi et al., Phys. Rev. D70 (2004) 074021, [hep-ph/0406302](#).
222. A.M. Kotzinian and P.J. Mulders, Phys. Lett. B406 (1997) 373, [arXiv:hep-ph/9701330](#).
223. H. Avakian et al., JLab Experiment C12-12-009 (2012).